方法として認識されつつある．しかしながらSentinel node conceptが食道癌で適応できるかどうかはまだcontroversialである．Katoらは92%(23/25)にsentinel nodeが検出可能であったと報告しているが[18]，sentinel node偽陰性2人で免疫染色で微小転移が確認され，現時点ではsentinel nodeだけの術中微小転移の検出で頸部郭清を決定するには，リスクが大きいと考えられる．

VII. 今後の問題点と展望

問題点として，リンパ節を2分割することから術中迅速HE陽性であるがRT-PCR陰性例である症例が存在することがあげられる．リンパ節全体をすべてRT-PCRに供すれば検出されるものと考えられるが，現時点では行っていない．SCCmRNAを標的としたRT-PCR単独よりCEAおよびCKもターゲットとした複数のRT-PCRを行うことにより検出漏れを防げるとする報告もあり[19]，今後検討を要する．また2時間半の検出時間は食道癌手術以外には術中検査としては長すぎる．最近，TRC(transcription reverse transcription concerted reaction)やLAMP(loop mediated isothermal amplification)法が微小転移検出に応用され始めており，今後の早期の導入に期待したい[20]．

また，われわれはマイクロアレイにより食道癌リンパ節転移責任遺伝子を同定し，ANN(artificaial neural network)を用いてリンパ節転移予測を行った．その結果，全例では24/28(86%)，test患者では10/13(77%)の予測率が得られ，test患者のうち2患者で微小リンパ節転移の予測が可能であった[21]．患者集積を重ねないと，まだ郭清範囲の決定に応用できる精度ではないが，将来はマイクロアレイも組み合わせてより精度の高い患者個別化治療ができるものと考えている．

おわりに

いくつかの施設で，同じような結果が得られており，コンセプトは正しいと考えているが，3領域郭清患者の個別化の意義は予後に反映されて初めて受け入れられるものと考えられる．われわれの短期予後は良好であるが，長期予後は観察期間が短くまだ評価できていない[15]．また，検討症例数も十分でないと考えている．したがって，今後も継続して症例を積み重ね，検証していかなくてはならない．

(謝　辞)

臨床研究部分は永谷史朗，角田　茂，東山元臣，伊丹　淳，渡辺　剛の協力により行われ臨床導入された．

文　献

1) Akiyama H, Tsurumaru M, Udagawa H, et al: Radical lymph node dissection for cancer of the thoracic esophagus. Ann Surg 220: 364-372, 1994.
2) Udagawa H, Akiyama H, Surgical treatment of esophageal cancer: Tokyo experience of the three-field technique. Dis Esophagus 14: 110-114, 2001.
3) Igaki H, Kato H, Tachimori Y, et al: Cervical lymph node metastasis in patients with submucosal carcinoma of the thoracic esophagus. J Surg Oncol 75: 37-41, 2000.
4) Tabira Y, Kitamura N, Yoshioka M, et al: Significance of three-field lymphadenectomy for carcinoma of the thoracic esophagus based on depth of tumor infiltration, lymph nodal involvement and survival rate. J Cardiovasc Surg (Torino). 40: 737-740, 1999.
5) Nishimaki T, Tanaka O, Suzuki T, et al: Patterns of lymphatic spread in thoracic esophageal cancer. Cancer 74: 4-11, 1994.
6) Sharma S, Fujita H, Yamana H, et al: Patterns of lymph node metastasis in 3-field dissection for carcinoma in the thoracic esophagus. Surg Today 24: 410-414. 1994.
7) Kato H, Tachimori Y, Watanabe H, et al: Lymph node metastasis in thoracic esophageal carcinoma. J Surg Oncol 48: 106-111. 1991.
8) Isono K, Sato H, Nakayama K: Results of a nationwide study on the three-field lymph node dissection of esophageal cancer. Oncology 48: 411-420, 1991.
9) Sato F, Shimada Y, Li Z, et al: Paratracheal lymph node metastasis is associated with cervical lymph node metastasis in patients with thoracic esophageal squamous cell carcinoma. Ann Surg Oncol 9: 65-70, 2002.
10) Tabira Y, Yasunaga M, Tanaka M, et al: Recurrent nerve nodal involvement is associated with cervical nodal metastasis in thoracic esophageal carcinoma. J Am Coll Surg 191: 232-237, 2000.
11) Shiozaki H, Yano M, Tsujinaka T, et al: Lymph node metastasis along the recurrent nerve chain is an indica-

tion for cervical lymph node dissection in thoracic esophageal cancer. Dis Esophagus 14 : 191-196, 2001.
12) Qubain SW, Natsugoe S, Matsumoto M, et al : Micrometastases in the cervical lymph nodes in esophageal squamous cell carcinoma. Dis Esophagus 14 : 143-148, 2001.
13) Shimada Y, Sato F, Maeda M, et al : Validity of intraoperative pathological diagnosis of paratracheal lymph node as a strategy for selection of patients for cervical lymph node dissection during esophagectomy. Dis Esophagus 16 : 246-251, 2003.
14) Kano M, Shimada Y, Kaganoi J, et al : Detection of lymph node metastasis of oesophageal cancer by RT-nested PCR for SCC antigen gene mRNA. Br J Cancer 82 : 429-435, 2000.
15) Nagatani S, Shimada Y, Li Z, et al : Validation of intraoperative detection of paratracheal lymph node metastasis using real-time RT-PCR targeting esophageal squamous cell carcinoma. Jpn J Clin Oncol 33 : 549-555, 2003.
16) Yoshioka S, Fujiwara Y, Sugita Y, et al : Real-time rapid reverse transcriptase-polymerase chain reaction for intraoperative diagnosis of lymph node micrometastasis : clinical application for cervical lymph node dissection in esophageal cancers. Surgery 132 : 34-40, 2002.
17) Nagatani S, Shimada Y, Kondo M, et al : A strategy for determining which thoracic esophageal cancer patients should undergo cervical lymph node dissection. Ann Thorac Surge 80 : 1881-1996, 2005.
18) Kato H, Miyazaki T, Nakajima M, et al : Sentinel lymph nodes with technetium-99m colloidal rhenium sulfide in patients with esophageal carcinoma. Cancer 98 : 932-939, 2003.
19) 嶋田 裕，永谷史朗，近藤正人ほか：食道癌微小転移による頸部郭清患者選択の妥当性の検証 第60回日本食道学会（東京）(2006. 7. 1)
20) 藤原義之，宮田博志，滝口修司ほか：術中迅速リンパ節転移診断法の新展開 臨床外科 59：593-599，2004.
21) Kan T, Shimada Y, Sato F, et al : Prediction of lymph node metastasis with use of artificial neural networks based on gene expression profiles in esophageal squamous cell carcinoma. Ann Surg Oncol 11 : 1070-1078, 2004.

外 科 治 療 第95巻・第3号

定価2,625円(本体2,500円＋税5％)（〒116円）
予約購読料 1年 37,600円（税込）
（増刊号を含む13冊／送料弊社負担）

発行日 —— 平成18年9月1日
編集兼発行人 —— 松 浦 三 男
印刷所 —— 日本写真印刷株式会社

発行所 —— 株式会社 永 井 書 店
〒553-0003 大阪市福島区福島8丁目21番15号
電話 06(6452)1881(代表)/FAX 06(6452)1882
振替口座 00980-7-121482
E-mail：geka@nagaishoten.co.jp
〒101-0062 東京都千代田区神田駿河台2-10-6

永井書店ホームページ
http://www.nagaishoten.co.jp

Int. J. Cancer: **118,** 230–242 (2006)

Cisplatin-dependent upregulation of death receptors 4 and 5 augments induction of apoptosis by TNF-related apoptosis-inducing ligand against esophageal squamous cell carcinoma

Kan Kondo[1]*, Seiji Yamasaki[2], Tomoharu Sugie[3], Naoki Teratani[1], Takatsugu Kan[1], Masayuki Imamura[1] and Yutaka Shimada[1]

[1]*Department of Surgery and Surgical Basic Science, Graduate School of Medicine, Kyoto University, Kyoto, Japan*
[2]*Department of Surgery, Murakami Memorial Hospital, Gifu prefecture, Japan*
[3]*Department of Surgery, Kyoto Police Hospital, Kyoto, Japan*

TNF-related apoptosis-inducing ligand (TRAIL) is a member of the TNF superfamily known to induce apoptosis in a variety of cancers. The purpose of our study was to examine the effects of TRAIL in combination with cisplatin against esophageal squamous cell carcinoma (ESCC) cell lines *in vitro* and *in vivo*, and to elucidate underlying molecular mechanisms. Expression profiles of TRAIL receptors were investigated in 19 ESCC (KYSE) cell lines using RT-PCR. Crystal violet staining assays were performed to reveal the sensitivity against TRAIL. Flow cytometric analyses of apoptosis induction and TRAIL receptor expression were performed. Furthermore, Western blot was used to clarify the apoptosis pathway involved, and a nude-mouse xenograft model was used to show effects *in vivo*. Results show that death receptors (DR) 4 and 5 were expressed in 100% of the cell lines, and 79% (15/19) expressed 4 TRAIL receptors. There was only 1 cell line without decoy receptor expression. Eighteen cell lines were resistant to TRAIL, but in some, the combination treatment with cisplatin could overcome this resistance. They underwent apoptosis *via* activation of caspase-8 and -3, and cisplatin-dependent upregulation of DR4 and 5 was detected. Furthermore, pretreatment with cisplatin followed by TRAIL resulted in significant tumoricidal effects. Finally, systemic administration of TRAIL with cisplatin synergistically suppressed tumor growth of ESCC xenografts in nude mice. These results provide a significance of cisplatin-induced upregulation of death receptors as apoptosis-inducing machinery, and it was suggested that sequential administration of cisplatin and TRAIL might be a feasible chemotherapeutic regimen against ESCC.

Key words: TNF-related apoptosis-inducing ligand (TRAIL); apoptosis; cisplatin; esophageal squamous cell carcinoma; chemotherapy

Esophageal SCC has extremely poor prognosis among gastrointestinal cancers because the diagnosis is not made until at an advanced stage and there are few effective therapies. Esophagectomy with extensive lymphadenectomy is far from being satisfactory with a dismal 5-year survival rate, and available chemotherapeutic regimens are yet to show promising outcomes. Thus, we are still in the midst of searching for a more effective modality to conquer this highly mortal malignancy.

TRAIL (also known as Apo2L) is a relatively new member of the TNF family that has been discovered from the expression sequence tag.[1,2] TRAIL is highly homologous to FasL and other members of the TNF ligand family, and its constitutive expression has been detected in a variety of human tissues including spleen, thymus, prostate, peripheral blood lymphocytes, ovary, small intestine, colon, placenta and lung, but not in the brain, liver or testis.[1] Four cognate receptors have been identified: death receptor (DR) 4 (TRAIL receptor (TR) 1)[3] and DR5 (KILLER/TR2[4–8] are receptors with fully functional cytoplasmic death domains. On the other hand, decoy receptor (DcR) 1 (TRID / TR 3)[4–6] and DcR 2 (TRUNDD / TR 4)[9–11] have either an obliterated (DcR1) or a truncated (DcR2) death domain. These decoy receptors have been proposed to competitively inhibit TRAIL-induced apoptosis by acting as nonfunctional receptors. All 4 TRAIL receptors are highly expressed in a wide variety of normal cells and the expression of decoy receptors is substantially limited in tumor cells.[3,5,10] These findings in addition to normal cells' resistance to TRAIL have lead to the presumptive belief that normal cells are protected from TRAIL-mediated apoptosis by decoy receptors[1,2,4,5,9,10] However, later studies revealed that DcR1 and DcR2 are also expressed in some cancers sensitive to TRAIL, thereby defying their putative function[12–15] Currently, exact functions of decoy receptors remain unknown and the mechanism for normal cells' resistance to TRAIL is still obscure. In the meantime, some studies raised questions regarding toxicity of TRAIL against normal tissues,[12,16] but this controversy seemed to be resolved by further findings that clinical-grade recombinant human TRAIL has minimal toxicity against normal human cells.[17,18]

Although TRAIL has been shown to be capable of inducing apoptosis in tumor cells of diverse origin,[19–23] studies on esophageal cancer have been very rare. In our study, ESCC cell lines (KYSE series) that have been established at our institution[24,25] are subjected to a series of experiments to demonstrate the potential usefulness of TRAIL against ESCC and underlying mechanisms behind this therapeutic model is discussed.

Material and methods

Cell lines

Nineteen genetically distinct KYSE cell lines were used. HeLa cells were used as positive controls for surface expression of DR4 and DR5 in flow cytometry. Peripheral blood mononuclear cells (PBMCs) isolated from whole blood of 2 of the authors (KK and NT) using Ficoll-Paque solution (Amersham Biosciences, London, UK) served as normal controls. All cells were cultured and maintained in RPMI 1640 (Nikken Biomedical Laboratory, Kyoto, Japan) plus 2% Fetal Bovine Serum (Biofluids, MD) at 37°C, in humidified 5% CO_2 atmosphere.

Patients

Original ESCC from which 19 KYSE series were established had been obtained during esophagectomy performed at the Department of Surgery and Surgical Basic Science of Kyoto University. All patients had a pathological diagnosis of squamous cell carcinoma, and their histological grading and staging were classified according to the pathological tumor/node/metastasis (pTNM) system (5th edition). The subjects consisted of 16 men and 3 women of age, 39–79 years (average age of 57.7 ± 9.8 years). There were no patients with distant organ metastasis, so all of the stage IV patients had distant lymph node metastasis. Details of patient characteristics are displayed in Table I. Written consent was obtained from the patients for the performance of surgery and for the use of

***Correspondence to:** Department of Surgery and Surgical Basic Science, Graduate School of Medicine, Kyoto University, Shogoin Kawaharacho 54, Sakyo-ku, Kyoto 606-8507, Japan. Fax: +81-75-751-4390 or +81-75-862-2312. E-mail: Terurin@kuhp.kyoto-u.ac.jp
Received 8 December 2004; Accepted after revision 27 April 2005
DOI 10.1002/ijc.21283
Published online 7 July 2005 in Wiley InterScience (www.interscience.wiley.com).

TABLE I – CLINICOPATHOLOGICAL CHARACTERISTICS OF 19 ORIGINAL TUMORS[1]

Parameter	n	Sensitivity to combination Tx		p Value
		+	–	
Age (years)				
<50	3	1	2	>0.999
>50	16	6	10	
Sex				
Female	4	2	2	= 0.603
Male	15	5	10	
N status				
N(+)	16	5	11	= 0.523
N(−)	3	2	1	
M status				
M(+)	5	2	3	>0.999
M(−)	14	5	9	
Tumor location				
Ce	4	1	3	= 0.930
Ut	3	1	2	
Mt	10	4	6	
Lt	2	1	1	
TNM stage				
2a	3	2	1	= 0.640
2b	2	0	2	
3	9	3	6	
4a	2	1	1	
4b	3	1	2	
Histological differentiation				
Well	6	1	5	= 0.365
Moderate	8	4	4	
Poor	4	2	2	

[1]Values represent numbers of patients except otherwise indicated.

resected samples for research in accordance with the Kyoto University Institutional Review Board.

Cytokines and antibodies

Soluble recombinant human TRAIL was purchased from DAKO (Denmark); cisplatin was obtained from Nippon Kayaku Co. Ltd. (Tokyo, Japan). Monoclonal mouse anti-caspase-8, anti-human BAX, anti-FADD and anti-XIAP antibodies were purchased from Medical & Biological Laboratories Co., Ltd (Nagoya, Japan). A monoclonal mouse anti-Bcl-X antibody, and polyclonal rabbit anti-caspase-8 and anti-caspase-3 antibodies were purchased from BD Pharmingen (San Diego, CA). A polyclonal rabbit anti-cFLIP antibody, a monoclonal mouse anti-β-actin antibody, and a mouse IgG1 isotype control were purchased from Sigma-Aldrich, Inc. (St. Louis, MO). A monoclonal mouse anti-FLIP antibody was purchased from Apotec (Geneva, Switzerland). Rabbit polyclonal anti-NFκB antibodies (anti-p50 and anti-p65) were purchased from Santa Cruz Biotechnology, Inc. (Santa Cruz, CA). Peroxidase-conjugated sheep anti-mouse IgG and donkey anti-rabbit IgG were purchased from Amersham Pharmacia Biotech (London, UK). Monoclonal mouse antibodies to TRAIL-R1, -R2, -R3, and -R4, and a biotinylated polyclonal antibody to mouse IgG1, were purchased from Alexis Biochemicals (UK). Streptavidin/FITC was purchased from Ancell Corporation (Bayport, MN).

Total RNA extraction and RT-PCR

Total RNA from KYSE cell lines was extracted using TRIzol reagent (Invitrogen, Carlsbad, CA) in accordance with the manufacturer's recommendations. PBMCs were incubated overnight in a 6-well tissue culture plate (Iwaki glass, Tokyo, Japan) before total RNA extraction. RNA quantification was performed spectrophotometrically. First strand cDNA was synthesized using 1 μg of total RNA, 1 μl of oligo $dT_{(12-18)}$ (Invitrogen), 4 μl of 5× first strand buffer (Invitrogen), 4 μl of dNTP mix (2.5 mM each) (Invitrogen) and 2 μl of 0.1 M DTT (Invitrogen), in a total volume of 20 μl. Previously published sequences of PCR primers were adopted: DR4 sense, 5′-CTG-AGC-AAC-GCA-GAC-TCG-CTG-TCC-AC-3′; DR4 antisense, 5′-AAG-GAC-ACG-GCA-GAG-CCT-GTG-CCA-T-3′;[26] DR5 sense, 5′-CTG-AAA-GGC-ATC-TGC-TCA-GGT-G-3′; DR5 antisense, 5′-CAG-AGT-CTG-CAT-TAC-CTT-CTA-G-3′[19] DcR1 sense, 5′-GTT-TGT-TTG-AAA-GAC-TTC-ACT-GTG-3′; DcR1 antisense, 5′-GCA-GGC-GTT-TCT-GTC-TGT-GGG-AAC-3′;[13] DcR2 sense, 5′-CTT-TTC-CGG-CGG-CGT-TCA-TGT-CCT-TC-3′; DcR2 antisense, 5′-GTT-TCT-TCC-AGG-CTG-CTT-CCC-TTT-GTA-G-3′;[26] glyceraldehyde-3-phosphate dehydrogenase (GAPDH) sense, 5′-TGG-TAT-CGT-GGA-AGG-ACT-CAT-GAC-3′ and GAPDH antisense, 5′-ATG-CCA-GTG-AGC-TTC-CCG-TTC-AGC-3′. PCR was performed using 5 μl of 10× PCR buffer (Sawady Technology, Tokyo, Japan), all 4 dNTPs at 2.5 mM, 2.5 U Taq DNA polymerase (Sawady Technology), 1/20 of cDNA and each primer at 0.5 μM, in a total volume of 50 mgr;l using PTC-200 Peltier thermal cycler (MJ Research, Inc., Watertown, MA). Thirty-five cycles of amplification were performed (melting step at 94°C for 1 min (DR4), 45 sec (DR5), 30s (DcR1), and 45 sec (DcR2); annealing step at 62°C for 1 min (DR4), 57°C for 45 sec (DR5), 56°C for 30 sec (DcR1), and 63°C for 45 sec (DcR2); elongation step at 72°C for 1 min (DR4), 45 sec (DR5), 30 sec (DcR1) and 45 sec (DcR2); followed by a final step at 72°C for 10 min). PCR product lengths were 505 bp (DR4), 583 bp (DR5), 140 bp (DcR1), 464 bp (DcR2) and 189 bp (GAPDH). Samples without reverse transcriptase served as negative controls to confirm that there was no genomic DNA contamination.

Crystal violet staining assay

Each cell line was cultured until subconfluent in 12-well tissue culture plates (Iwaki glass), and TRAIL (0 ng/ml, 50 ng/ml or 100 ng/ml) and cisplatin (0 μg/ml, 2.5 μg/ml or 5 μg/ml) were added either alone or in combinations for 24 hr. Then medium was discarded and adherent cells were washed with PBS, stained and fixed with 0.2% crystal violet in 10% phosphate-buffered formaldehyde (Wako Pure Chemical, Japan) for 30 sec. Excess crystal violet solution was discarded, and adherent cells, considered viable, were observed. After completely air-dried, stained cells were lysed with 2% SDS solution by shaking plates in room temperature for 1 hr. OD absorbance was measured at 560 nm using SJeia II microplate reader (Sanko Jun-yaku Co., Ltd., Tokyo, Japan), and the percent absorbance of every well was determined.

Flow cytometry for detection of apoptotic cells and surface TRAIL receptor expression

KYSE cell lines, HeLa cell line (5×10^5 cells) and PBMCs (3×10^6 cells) were seeded in 24-well tissue culture plates (Iwaki glass). For detection of apoptosis, TRAIL (50 ng/ml) and cisplatin (5 μg/ml) were added either alone or in combination for 24 hr. Subsequently, floating cells in the medium and adherent cells were collected. Using Annexin V-FITC Apoptosis Detection Kit (Medical & Biological Laboratories Co., Ltd.), cells were stained with Annexin-V FITC and propidium iodide (PI) according to manufacturer's instructions. Untreated cells and cells treated with 3% formaldehyde for 30 min served, respectively, as negative and positive controls for double staining. For detection of surface TRAIL receptor expression, cells were either untreated (control) or treated with 5 μg/ml cisplatin for 6 hr, harvested, and stained with monoclonal antibodies against TR1–TR4, followed sequentially by incubation with biotinylated goat anti-mouse IgG, and then with streptavidin-FITC. HeLa cells served as positive controls for DR4/5 surface expression, and PBMCs served as positive controls for DcR1/2 surface expression. Cells were analyzed immediately after staining using a FACScan flow cytometer (Becton Dickinson, Mountain View, CA) and the Cell Quest software (Becton Dickinson). For each measurement, >10,000 cells were counted.

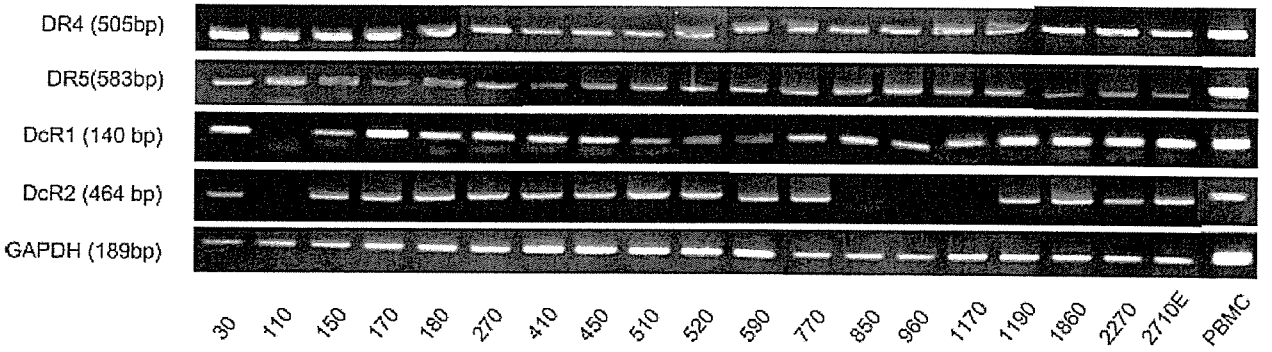

FIGURE 1 – RT-PCR detection of TRAIL receptors in 19 KYSE cell lines and peripheral blood mononuclear cells (PBMCs): RT-PCR was run for 35 cycles. DR4 and DR 5 were expressed in all cell lines. Four cell lines lacked DcR2 expression, and KYSE 110 was the only decoy receptor (−) cell line. Glyceraldehyde-3-phosphate dehydrogenase (GAPDH) expression is shown as a loading control. Experiments were repeated at least 3 times and the most representative results are shown.

Morphological analysis using Hoechst33342 and propidium iodide staining

In some cell lines, nuclear morphology was assessed using Hoechst 33342 and PI staining. After 24 hr treatment with TRAIL and cisplatin, cells were harvested, labeled with Hoechst 33342 (5 μg/ml) and PI (1 μg/ml) at 37°C for 10 min and examined under fluorescent microscopy according to the method reported previously.[27] Intact blue nuclei, condensed/fragmented blue nuclei, condensed/fragmented pink nuclei and intact pink nuclei were considered viable, early apoptotic, late apoptotic and necrotic cells, respectively.

Immunoblotting analyses

Lysis buffer containing 2% SDS solution supplemented with Tris-HCl, pH 6.5 and 25% glycerol, and a mixture of protease inhibitors in DMSO solution (Wako Pure Chemicals) was used to destruct cellular structures. Lysates were then sonicated on ice, centrifuged and protein concentration determined using BCA protein assay kit (Pierce, Rockford, IL). Next, Sodium dodecyl sulfate-polyacrylamide gel electrophoresis (SDS-PAGE) was performed using 12.5% (w/v) gel, followed by transblotting to Immobilon-P transfer membranes (Millipore, Bedford, MA). Nonspecific bindings were blocked using Blockace solution (Dainippon Pharmaceutical Co., Osaka, Japan), and incubation with primary antibodies was carried out. After washing 3 times with tris-buffered saline with Tween 20, pH 8.0 (0.05 M Tris, 0.138 M NaCl, 0.0027 M KCl and 0.05% Tween 20; Sigma-Aldrich), the membrane was successively incubated with secondary antibodies and peroxidase activity was revealed using an ECL plus chemiluminescence kit (Amersham Pharmacia Biotech).

Combination treatment with sequential addition of TRAIL and cisplatin

KYSE cell lines sensitive to the combination treatments were cultured to subconfluence in 12-well tissue culture plates and 50 ng/ml TRAIL and 5 μg/ml cisplatin were added sequentially either TRAIL first, washed 3 times with PBS and then cisplatin, or *vice versa*, for 12 hr each. Crystal violet staining assays were then performed.

In vivo *treatments*

KYSE 170 cells (5×10^6) were suspended in 100 μl PBS and inoculated subcutaneously into the right flank of the female nude mice, 5–6 weeks of age, of BALB/c background (Charles River Japan, Inc., Kanagawa, Japan). For the treatment of the established xenografts, the tumors were permitted to establish to the diameter of 6–7 mm for 10–14 days. Either cisplatin (1 mg/kg, 2 mg/kg, or 3 mg/kg), sterile normal saline (150 μl/body), or TRAIL (1 μg/body) was administered intraperitoneally (i.p.) daily for 4 consecutive days followed by 3 off-days per 1 course of a treatment. For the combination treatment, 2 mg/kg cisplatin and 1 μg/body-TRAIL were administered i.p. in the same dose schedule. Mice in all groups were treated for 2 consecutive weeks and then observed. Tumor growth was followed by measurements of tumor diameters with a sliding caliper 3 times a week, and mice were monitored daily. The tumor volume was calculated according to the following formula: $TV = L \times W^2/2$, where L and W are the major and minor dimensions, respectively. Systemic toxicity of the treatments was assessed by change in body weights. All treatment protocols were approved by the animal care and use committee of Kyoto University.

Statistical analyses

Commercially available software, Stat View version 4.5 (Berkeley, CA), was utilized for all statistical analyses. The correlations between various clinicopathological factors and sensitivity to the combination therapy were evaluated using Fisher's exact test and Kruskal-Wallis test. ANOVA Bonferroni test was used to evaluate the significance of differences in rates of apoptosis induction between combination therapies and single drug therapies. Mann-Whitney U-test was used to analyze the significance of difference of tumoricidal effects of the sequential treatment. In all tests, p values less than 0.05 were considered significant.

Results

TRAIL receptor expression profiling in KYSE cell lines and PBMCs

A summary of RT-PCR results on 19 KYSE cell lines and PBMCs is shown in Figure 1. DR4 and DR5 expression was detected in all of the cell lines; thus, they were ubiquitously expressed among KYSE cell lines. DcR1 was expressed in 18 of 19 cell lines (95%) and DcR2, in 15 of 19 cell lines (79%). There was only 1 cell line (KYSE 110) that was completely devoid of the decoy receptor transcripts. All 4 TRAIL receptor transcripts were detected in PBMCs.

Tumoricidal effects of TRAIL and cisplatin against KYSE cell lines

KYSE 110, 170 and 520 were subjected to the preliminary crystal violet staining assays. They had been selected because KYSE 110 is our only decoy-receptor negative cell line, and KYSE 170 and 520, which express all 4 TRAIL receptors, are 2 of the most frequently studied cell lines in our laboratory.[25,28] KYSE 110 and 170 were sensitive to the combination treatments, while KYSE 520 appeared to be resistant (Fig. 2*a*). Reduction of viable KYSE 110 and 170 cells by the treatment using 50 ng/ml TRAIL and 5 μg/ml cisplatin was statistically significant compared to either

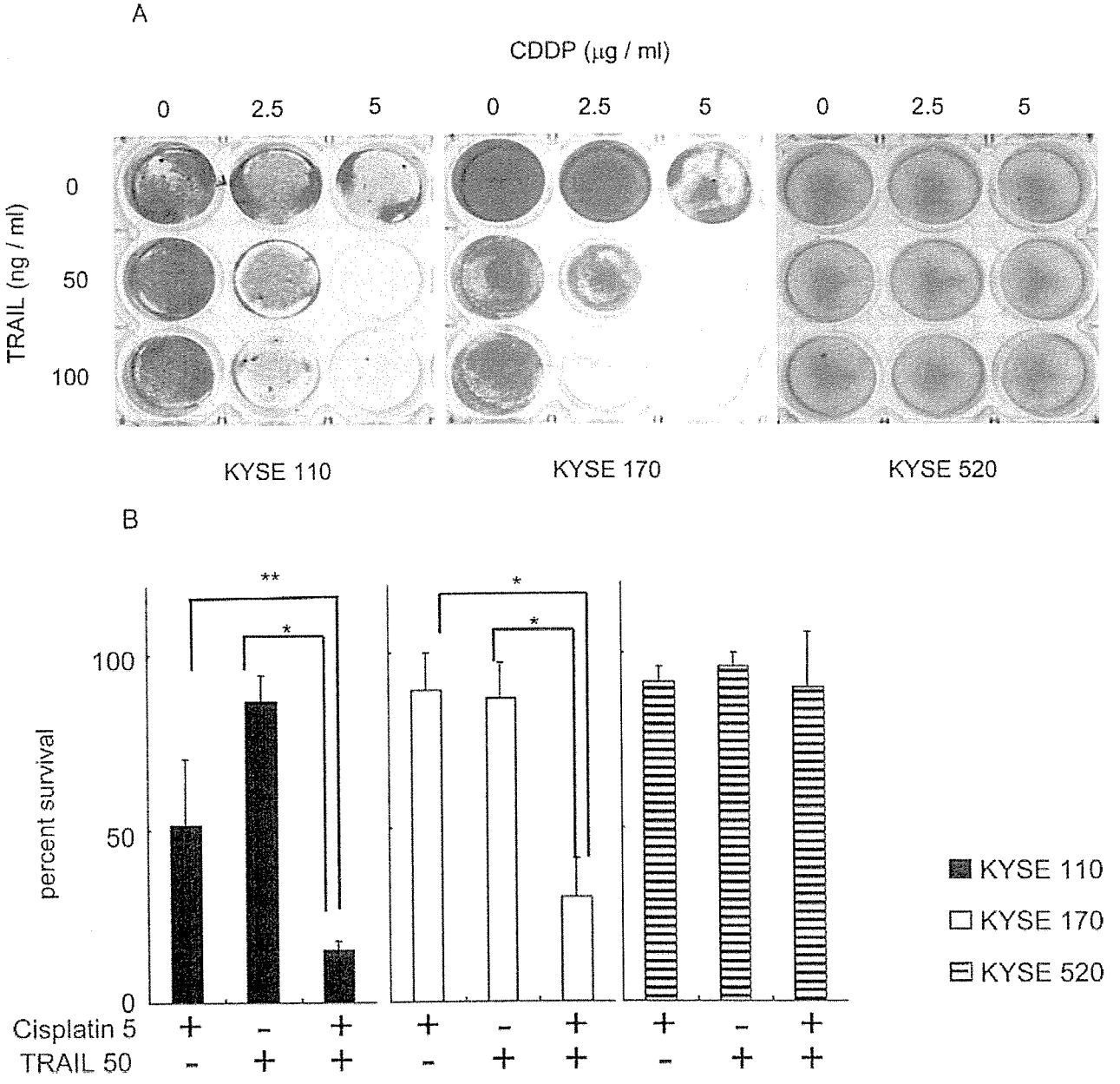

FIGURE 2 – (*a*) Crystal violet staining results after treatments with various concentrations of TRAIL and cisplatin for 24 hr are shown. KYSE 110 and KYSE 170 were sensitive to combination treatments, whereas KYSE 520 was resistant. Experiments were repeated 6 times per cell line, and the most representative results are shown. (*b*) Crystal violet staining results were quantified with OD absorbance. For each cell line, OD absorbance value for untreated control was arbitrarily set for 100%. All data are the mean of 4 independent experiments; bars represent SE. Cytotoxic effects in both KYSE 110 and KYSE 170 by the combination treatment was statistically significant compared to either single agent alone (*$p < 0.001$. **$p < 0.05$).

single agent alone, displaying synergistic effects (Fig. 2*b*). Hence, 50 ng/ml TRAIL and 5 μg/ml cisplatin were adapted to pursue further studies. Among 19 KYSE cell lines, KYSE 110, 170, 510, 850, 1190, 1860 and 2270 showed variable levels of sensitivity against the combination treatment and KYSE 2270 was the only cell line sensitive to TRAIL alone (Fig. 3). In the subsequent studies, KYSE 110 170, 1860 and 2270 had been selected because in these cell lines, viable cells were reduced significantly by the combination treatment, compared to either single agent alone. KYSE 960 and 1170 were used as resistant cell lines that lack DcR2 expression.

Apoptosis induced by the combination treatment in KYSE cell lines

To assess the type of cell death induced by TRAIL and cisplatin, flow cytometry was performed; Annexin-V binds to cells that express phosphatidylserine on the outer layer of the cell membrane, and PI stains the cellular DNA of cells with a compromised cell membrane. This allows for the discrimination of live cells (unstained) from early apoptotic cells (stained only with annexin-V) and late apoptotic or necrotic cells (stained with both annexin-V and PI). Cisplatin alone could induce a notable level of apoptosis only in KYSE 1860 (4.7% control *vs.* 30.8%) (Fig. 4*a*).

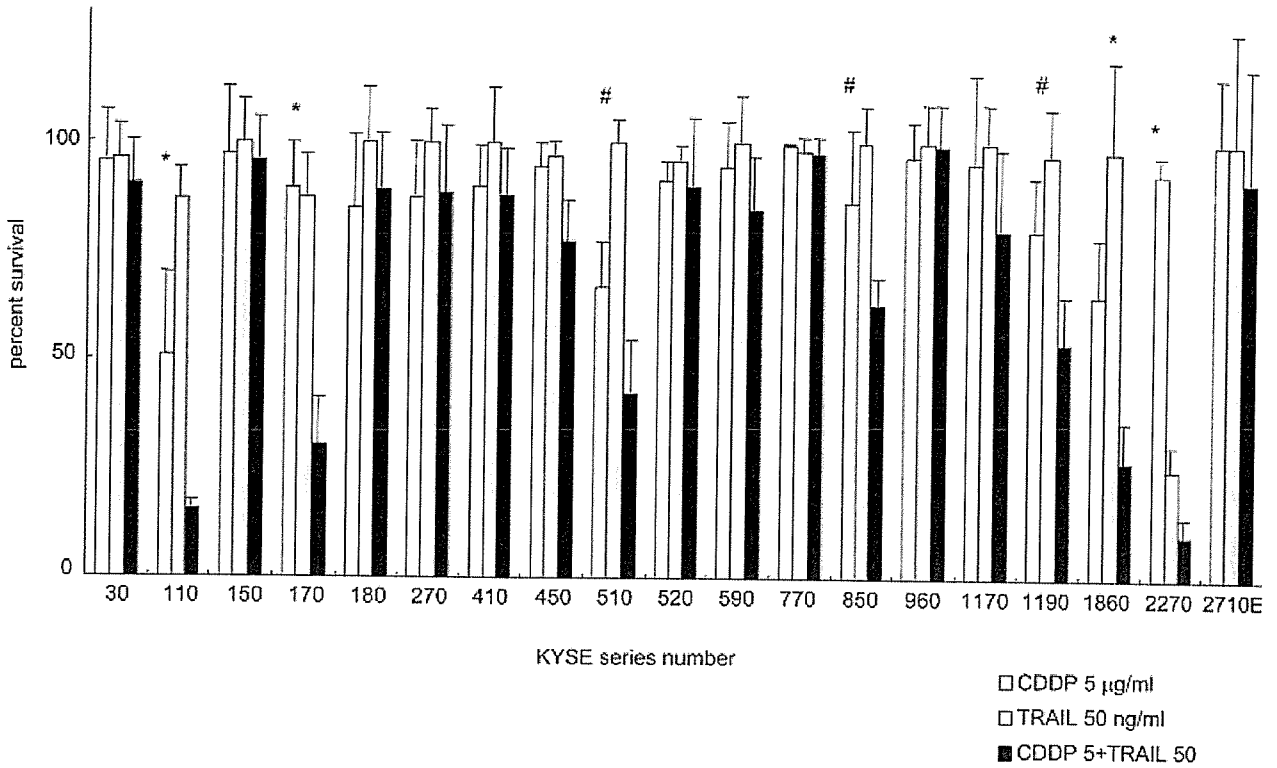

FIGURE 3 – After in contact with given doses of TRAIL and cisplatin for 24 hr, sensitivities of 19 KYSE cell lines to these agents either alone or in combination were evaluated with the crystal violet staining assays. Three cell lines (KYSE 110, 510 and 1860) and 1 cell line (KYSE 2270) showed some sensitivities to cisplatin and TRAIL, respectively. With the combination treatment, variable levels of cytotoxic effects were seen in 7 cell lines (KYSE 110, 170, 510, 850, 1190, 1860 and 2270). Asterisk indicates the cell lines in which cytotoxicity by the combination treatment was statistically significant ($p < 0.05$) compared to either single agent alone. Number sign denotes the cell lines in which cytotoxicity induced by the combination treatment was statistically significant compared to 1 of the 2 agents. Results indicate the mean of 4 independent experiments for each cell line.

TRAIL alone induced extensive apoptosis in KYSE 2270 (7.7% control *vs.* 88.5%) and some apoptosis in KYSE 170 (14.6% control *vs.* 35.3%) and 1860 (4.7% control vs. 21.9%). KYSE 110, despite absence of decoy receptors, did not undergo significant apoptosis when treated with TRAIL alone. However, the combination treatment resulted in synergistic cytotoxic effects. A majority of apoptotic cells in KYSE 110 was in early apoptosis while those in KYSE 170, 1860 and 2270 were in late apoptosis. By extending treatment periods to 48 hr, however, most of the apoptotic cells in KYSE 110 proceeded to a late apoptotic stage, revealing relatively slow progression of apoptotic process in KYSE 110 (data not shown). On the contrary, there was hardly any increase of apoptotic cells in KYSE 410, 520, 960 and 1170 (Fig. 4*b*), and these results were comparable with those in crystal violet assays. To further confirm that KYSE 170, 1860 and 2270 underwent apoptosis by the combination treatment, nuclear morphology was observed under fluorescent microscope, which revealed cells either in early or late apoptosis, but not in necrosis (Fig. 5). Meanwhile, PBMCs were resistant to both TRAIL and cisplatin, and the combination treatment could not induce apoptosis either (Fig. 4*b*).

Demographic data analyses

Clinicopathological data of 19 original ESCC are shown in Table I. Parameters compared are age and gender of the patients, TNM status, location of the primary tumor, TNM stage and histological grading of the resected tumor, against sensitivity to the combination treatment of TRAIL and cisplatin. In 1 of the patients, histological grading was not available. Although significant statistical differences could not be reached between cell lines sensitive to, and resistant to, the combination treatment in any of the criteria examined, well-differentiated SCC tended to be more resistant to the combination treatment, as 5 of 6 (83.3%) well-differentiated tumors were resistant, as opposed to 6 of 12 (50%) moderately and poorly differentiated tumors ($p = 0.316$).

Activation of caspase cascade by the combination treatment

TRAIL is known to induce apoptosis in target cells *via* activation of the caspase cascade (extrinsic pathway).[15,29] It has also been disclosed that caspase-8 can activate Bid of the Bcl-2 family to initiate the mitochondrial (intrinsic) pathway of apoptosis.[20,30,31] To unveil the TRAIL-mediated apoptosis pathway in KYSE cell lines, the expression of pro-apoptotic proteins caspase-8, -3, Bax, FADD and anti-apoptotic proteins Bcl-XL, FLIPL and XIAP has been investigated. First, in order to determine the optimal timing of protein extraction, KYSE 170 was treated with TRAIL and cisplatin, proteins extracted every 2 hr and activation of caspase-8 examined. An active form of caspase-8 was detectable within 4 hr and appeared to peak at 8 hr; hence, 8 hr contact time was deemed sufficient for protein extraction (Fig. 6). The baseline expression levels of these proteins in untreated controls are shown in Figure 7*a*. The expression levels of FADD, FLIPL and XIAP were variable among cell lines but there was no correlation between their expression levels and cell lines' sensitivity to the combination treatment. After the combination treatment, activation of caspase-8 and -3 was observed in KYSE 110, 170, 1860 and 2270 but not in KYSE 410, 520, 960 and 1170 (Fig. 7*b*). In order to elucidate intracellular changes involved in cisplatin-induced sensitization of esophageal SCC, Western blotting detection of FLIPS, FLIPL, XIAP and NFκB was further performed on both untreated cells and cells treated with 5 μg/ml cisplatin for

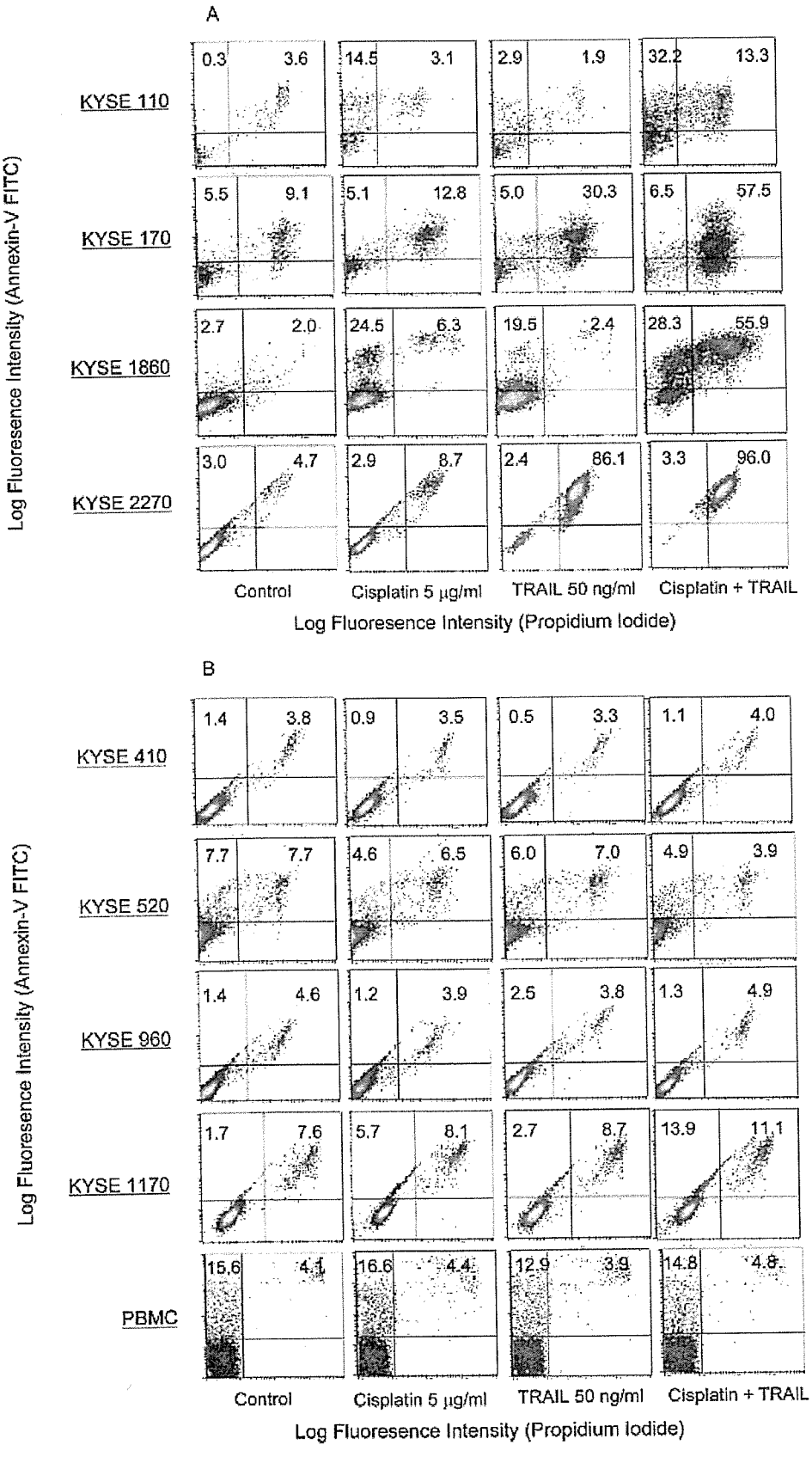

FIGURE 4 – Flow cytometric detection of apoptotic cells: Concentration of each agent used for "cisplatin + TRAIL" is 5 μg/ml and 50 ng/ml, respectively. Y-axis: Annexin-V conjugate. X-axis: Propidium Iodide uptake. Lower left quadrant, upper left quadrant, and upper right quadrant represent viable cells, cells in early apoptosis, and cells in late apoptosis respectively. Numbers in the diagrams show the percentage of cells represented in respective quadrants. (*a*) Cell lines sensitive to the combination treatment. Enhanced induction of apoptosis by the combination treatment was clearly observed in KYSE 110, 170, 1860 and 2270. B, KYSE 410, 520, 960, 1170 and PBMCs were resistant to the combination treatment and did not undergo apoptosis. Experiments were repeated at least 3 times for each cell line, and the most representative results are shown.

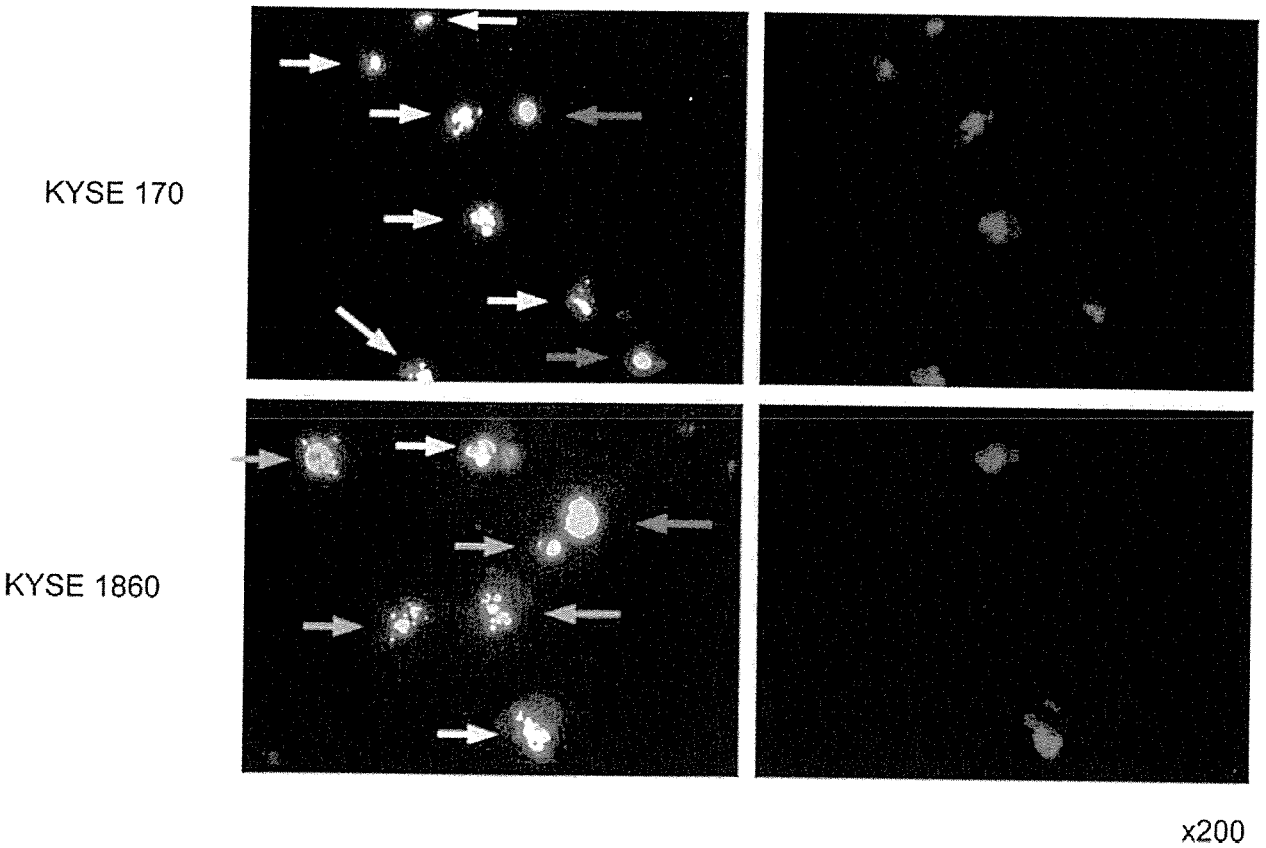

FIGURE 5 – Results of the morphological analyses of the nucleus using Hoechest 33342 and propidium iodide (PI) performed on KYSE 170 and 1860 after they had been treated with 50 ng/ml TRAIL and 5 μg/ml cisplatin for 24 hr. Left panels show Hoechest 33342 and PI staining. Right panels show the same view of the PI staining only. Most cells are either in early or late apoptosis, and necrotic cells were rather scarce. Intact blue nuclei (red arrow), condensed/fragmented blue nuclei (green arrow), condensed/fragmented pink nuclei (yellow arrow) and intact pink nuclei (not seen in the figure) represent viable, early apoptotic, late apoptotic and necrotic cells, respectively.

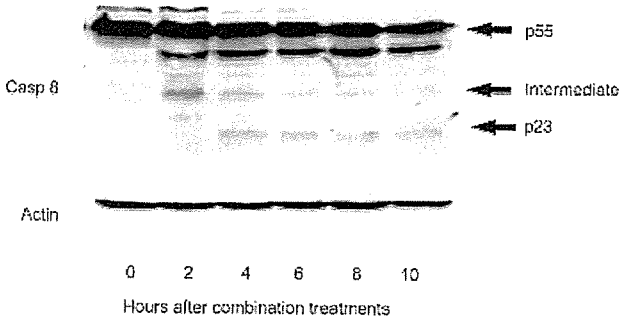

FIGURE 6 – Activation of procaspase-8 in KYSE 170. Cells were treated with TRAIL and cisplatin for indicated hours, and cell lysates were obtained for immunoblotting. An intermediate product of caspase-8 started to appear after 2 hr, and an active form was observable after 4 hr. Detection of the active form appeared to peak after 8 hr. Beta-actin expression is shown as a loading control. Experiments were repeated 3 times, and the most representative results are shown.

8 hr. Results are shown in Figure 7*c*. All 8 cell lines expressed FLIPL, FLIPS , XIAP and NFκB in various levels, and direct correlation between expression levels of these proteins and cell lines' sensitivity to the combination treatment was not apparent. However, slight decreases in expression levels of XIAP and FLIPS were noted in sensitive cell lines after the cisplatin treatment while their expression levels remained unchanged in the resistant cell lines. Meanwhile, expression levels of NFκB (p50, p65 and p115) and FLIPL remained unaffected by the cisplatin treatment (Fig. 7*c*).

Cisplatin-induced upregulation of DR4 and DR5 in KYSE cell lines

Influences of cisplatin on the surface expression of TRAIL receptors in KYSE cell lines were next investigated by flow cytometry, which clearly showed cisplatin-induced upregulation of both DR4/5 expression in KYSE 110, 170,1860 and 2270 after 6 hr exposure (Fig. 8*a*). On the other hand, their expression levels in KYSE 410, 520, 960 and 1170 remained nearly unchanged (Fig. 8*b*). Expression of the surface DcR1/2 paralleled that of mRNA transcripts but neither cisplatin-dependent upregulation nor downregulation was observed in any of the cell lines (Fig. 8*b*). Similar experiments were performed with PBMCs; DR4 was not detected on the surface of PBMCs even though DR4 mRNA was present by RT-PCR. DR5, DcR1 and DcR2 were detectable, but their expression levels were not influenced by the exposure to cisplatin.

Sensitization of KYSE cell lines to TRAIL by pretreatment with cisplatin

From the results thus far, upregulation of DR4/5 by cisplatin may be a critical factor rendering cells sensitive to the combination treatment. To confirm this, crystal violet staining studies were carried out in sensitive cell lines by sequentially adding cisplatin and TRAIL. Since KYSE 2270 was sensitive to TRAIL, signifi-

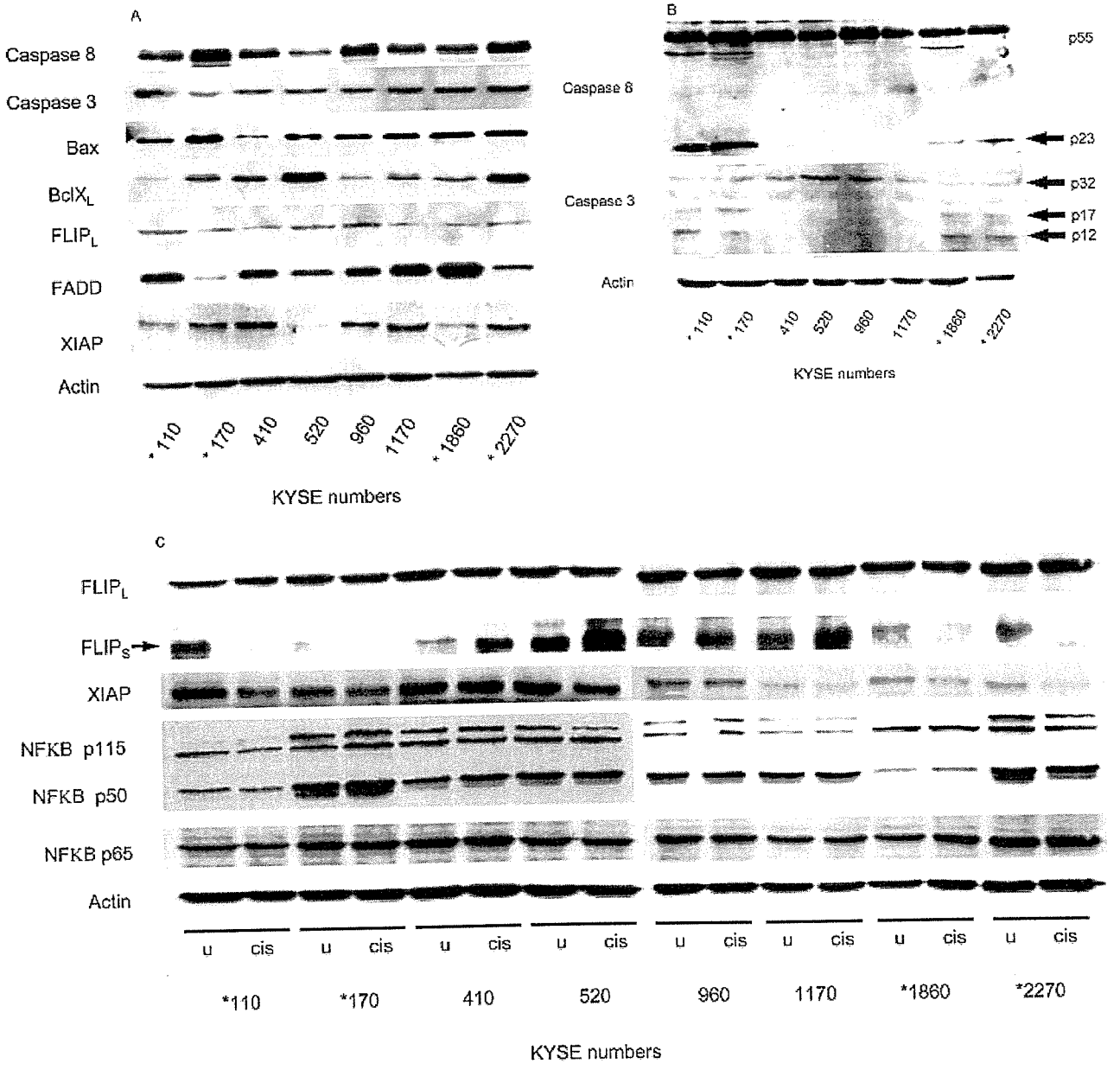

FIGURE 7 – Detection of key apoptotic proteins by immunoblotting analyses: (*a*) in untreated cells, procaspase-8, procaspase-3, Bax, Bcl-XL, cFLIP, FADD and XIAP were expressed in all 8 cell lines. The numbers below the figure represent the cell line numbers. (*b*) Eight hours after the combination treatment with TRAIL and cisplatin, proteolytic activation of procaspase-8 and procaspase-3 were observed in sensitive cell lines KYSE 110, 170, 1860 and 2270 but not in resistant cell lines KYSE 410, 520, 960 and 1170. (*c*) Eight hours after the treatment with 5 μg/ml cisplatin, slight decreases in expression level of anti-apoptotic proteins XIAP and FLIPS were observed in sensitive cell lines. Expression levels of NFκB (p115, p65 and ad p50) remained unchanged. u: untreated samples, cis: samples treated with 5 μg/ml cisplatin, p55: Procaspase-8, p23: cleaved caspase-8, p32: Procaspase-3, p17/p12: cleaved caspase-3. Beta-actin expression is shown as a loading control. Experiments were repeated at least 3 times, and the most representative results are shown. Asterisk denotes cell lines sensitive to the combination treatment.

cant cytotoxicity was observed regardless of the treatment sequence, but in other 3 cell lines, pretreatment with cisplatin followed by treatment with TRAIL resulted in significantly more cytotoxic effects than when the sequence was reversed (Fig. 9).

In vivo *suppression of tumor growth by the treatment of nude mice with TRAIL and cisplatin*

Because cisplatin enhanced the apoptosis-inducing potential of TRAIL by upregulating DR4/5 *in vitro*, we sought to examine whether this combination is effective in an established ESCC tumor model *in vivo*. KYSE 170 was implanted into the right thigh of the nude mice. Similar to *in vitro* experiments, TRAIL and cisplatin were simultaneously injected i.p. to observe their effects. KYSE 170 tumors carried by mice treated with the combination of TRAIL and cisplatin grew slower after the first course of treatment and remained smaller than any other tumors except those treated with 3 mg/kg cisplatin (Fig. 10*a*). In contrast, tumors in mice treated with normal saline or with TRAIL singly grew significantly faster. The suppression of tumor growth by the combination

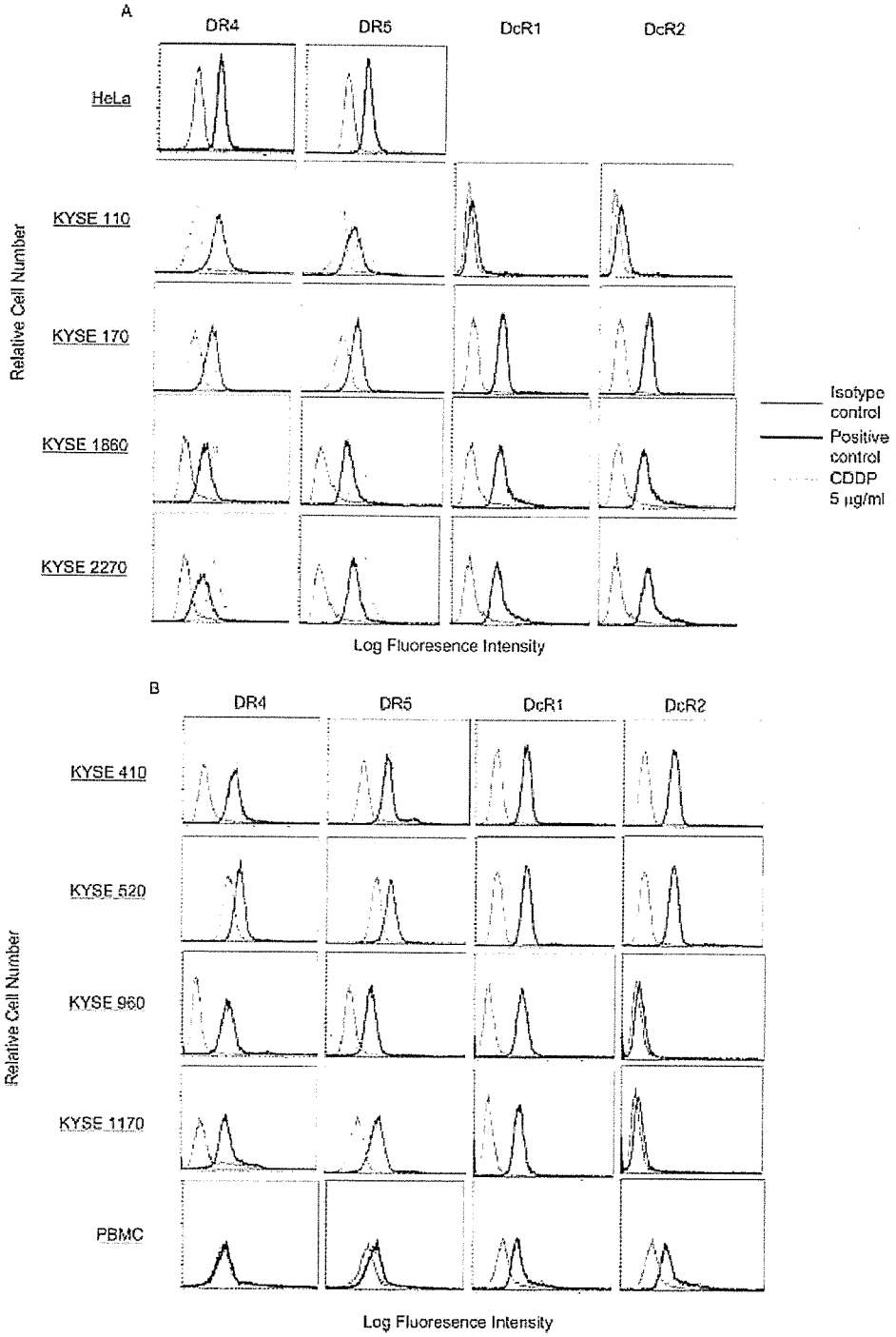

FIGURE 8 – Flow cytometric analysis of surface DR4 and DR5 expression. (*a*) Cell lines sensitive to the combination treatment. (*b*) Cell lines resistant to the combination treatment. HeLa cells served as the positive control for the surface expression of DR4 and DR5. PBMCs served as the positive control for DcR1 and DcR2. The baseline expression patterns of TRAIL receptors in KYSE cell lines paralleled those of the mRNA transcripts. In PBMCs, however, the surface expression of DR4 could not be detected. The cell lines sensitive to the combination treatment revealed cisplatin-induced upregulation of both DR4 and DR5 but in the resistant cell lines including PBMCs, expression levels of DRs was unaffected. Expression of decoy receptors was not influenced by the addition of cisplatin in any of the cell lines. Experiments were repeated at least 3 times for each cell line, and the most representative results are shown.

treatment was statistically significant compared to TRAIL alone ($p = 0.0006$) or normal saline ($p < 0.0005$), but the statistical significance was not reached when compared to the effect of 2 mg/kg cisplatin ($p = 0.253$). On the contrary, weight loss of the mice treated with 3 mg/kg cisplatin was much more than mice in any other groups, though statistical significance was not reached (Fig. 10*b*). Both the suppression of tumor growth and weight loss of mice were dose dependent for cisplatin, but the addition of TRAIL did not appear to influence the weight of mice, consistent with other reports that TRAIL causes minimal or no side effects in mice.[19,32]

Discussion

The present results indicate that ESCC cell lines are generally resistant to TRAIL, but in some cell lines that resistance can be overcome by adding cisplatin. Death signals originate from the

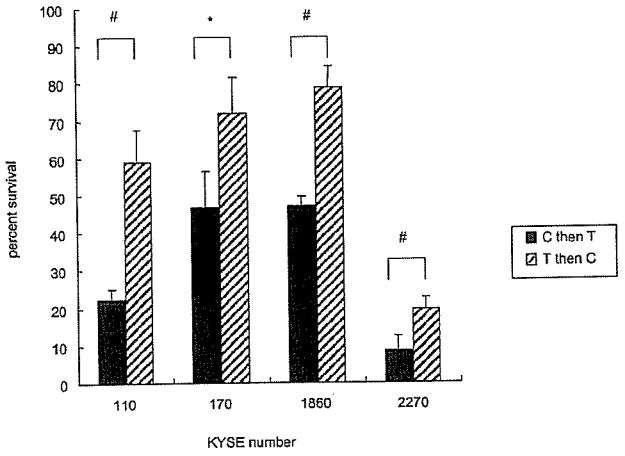

FIGURE 9 – KYSE 110, 170, 1860 and 2270 were subjected to the sequential administration of cisplatin and TRAIL. They were either pretreated with 5 μg/ml cisplatin for 12 hr, followed by treatment with 50 ng/ml TRAIL for 12 hr (C then T), or *vice versa* (T then C), stained with the crystal violet solution and OD absorbance was measured. OD absorbance of untreated cells was set for 100%. For all 4 cell lines, pretreatment with cisplatin followed by TRAIL resulted in statistically significant cytotoxic effects compared to the reverse sequence. KYSE 2270, which is sensitive to TRAIL, revealed significant cytotoxicity regardless of the treatment sequence. Graphs represent the mean of 8 independent experiments for each cell line; bars, SE. $\#p < 0.001$. $*p < 0.005$.

TRAIL receptors and we have demonstrated that cisplatin can upregulate DR4/5 to enhance ligand-induced cytotoxicity. All KYSE cell lines expressed both DR4 and DR5, showing a quintessential pattern of death receptor expression in malignant cell lines. The decoy receptors had been thought to play a cytoprotective role against TRAIL in normal cells[4–6,9,10] until TRAIL-sensitive tumors expressing decoy receptors were reported[13,14,20,29,33] to keep their roles remain ambiguous. When compared to other tumor cell lines, incidences of DcR1/2 expression in KYSE cell lines are higher than expected, with only 1 decoy-receptor negative cell line. High incidences of decoy receptor expression may be one of the unique molecular characteristics reflecting TRAIL-resistant nature of ESCC.

Statistical analysis of clinicopathological data of the original cancers revealed that sensitivity to the combination treatment was unrelated to age, gender, location of the tumor, lymph node metastasis, distant lymph node metastasis or TNM staging of the tumor. However, although statistical significant was not reached, well-differentiated ESCC tended to be more resistant to the combination treatment compared to moderately and poorly differentiated ESCC. One of the possible explanations for this is that well differentiated ESCC retains more characteristics of normal esophageal epithelial cells. Since normal cells are generally resistant to TRAIL, well-differentiated ESCC might remain more resistant to the treatment with TRAIL. Furthermore, although statistical significance was not reached, 100 % of the well-differentiated tumors expressed both DcR1 and DcR2 whereas some of the moderately and poorly differentiated tumors lacked decoy receptor expression. By increasing the number of samples, resistant characteristics and differences in expression levels of decoy receptors may become more evident.

Several chemotherapeutic agents including cisplatin, one of the most common anticancer drugs against ESCC, have been reported to upregulate DR4/5 to augment TRAIL-mediated apoptosis in cancer cells.[19,21,22,32] Consequently, we selected cisplatin to evaluate whether or not it can break TRAIL resistance in ESCC. Although cisplatin alone was largely ineffective at the given dose, when combined with TRAIL, synergistic cytotoxicity was exerted in 7 out of 19 (37%) cell lines. Further examination revealed that the addition of cisplatin did not influence decoy receptor expression, but it was rather capable of upregulating DR4/5 to augment TRAIL-mediated apoptosis. Following the time course of death receptor upregulation in these cell lines with flow cytometry, they became clearly bright after 6 hr, but even after the 4 hr contact, the upregulation seemed to have begun (data not shown). These results demonstrated that upregulation of DR4/5 by cisplatin begins relatively early in the sensitive cell lines. However, DR expression of the resistant cell lines was not affected. Several different mechanisms have been suggested for upregulation of DRs. Sheikh *et al.*[34] has shown the involvement of p53 at the transcriptional level in upregulation of DR5, and Gibson *et al.*[22] has suggested differential activation of NFκB could upregulate both DR4 and DR5. Still others suggested the involvement of post-translational mechanisms such as stabilization of cellular microtubules,[35] differential translocation of intracellularly stored DRs upon stimulation by the chemotherapeutic agents[33,36] and chemotherapeutic agent-mediated changes in the rate of receptor turnover at the cell surface.[37] Since none of the mechanisms could sufficiently explain DR upregulation in all of the cancers, this mechanism might differ in different types of cancer. In our study, semiquantitative RT-PCR performed on KYSE 110 and 170 also revealed upregulation of DR4/5 transcripts after the treatment with 5 μg/ml cisplatin (data not shown); therefore, an increase in mRNA transcription may be responsible for DR upregulation in ESCC. Interestingly, in PBMCs, DR4 was not expressed on the surface even though DR4 mRNA was detected in RT-PCR, while surface DR5, DcR1 and DcR2 were expressed, as were their respective mRNA transcripts. The expression of these receptors was not influenced by cisplatin. These results indicate that deficient DR4 expression and lack of DR upregulation in addition to the decoy receptors might contribute to PBMCs' resistance to the combination treatment. It appears that the control of DR4 expression is at the post-transcriptional level in PBMCs, and differs from ESCC. Overall, it may be deduced that the induction of death receptor upregulation by cisplatin in esophageal SCC is indicative of their sensitivity to the combination treatment with TRAIL.

In ESCC, DcR1 and DcR2 do not seem to be essential with regard to their sensitivity against TRAIL for following 2 reasons. First, KYSE 110, the decoy receptor negative cell line, is resistant to TRAIL itself. Second, some of the decoy receptor positive cell lines became susceptible to TRAIL in the presence of cisplatin even though their expression of DcR1 and DcR2 are not influenced by cisplatin. It appears that physiological expression levels of DcR1 and DcR2 are not sufficient to interfere with TRAIL-induced apoptosis as was demonstrated in overexpression experiments of the initial reports investigating TRAIL receptors.[3,6,9,13,14,20,29,33] Furthermore, although a possible role of DcR2 as a NFκB activator has been disclosed,[11] functional roles of DcR1 is yet to be elucidated. Taken together, it seems unlikely that signals originating from DcR1/2 upon binding of TRAIL overcome those from DR4/5 in ESCC to inhibit TRAIL-mediated apoptosis, and the mechanisms of TRAIL resistance seemingly resides on the intracellular factors rather than DcR1 and DcR2.

Apoptosis-inducing mechanisms by TRAIL is thought to be similar to its kin, FasL and TRAIL-mediated apoptosis *via* the extrinsic pathway has been delineated by Griffith *et al.* and others.[15,20,23,29] While TRAIL receptor-specific cytoplasmic adapter protein is yet to be discovered, some studies have reported that FADD may act as the adapter protein for TRAIL receptors.[38] Our study clearly indicated the involvement of caspases in TRAIL-mediated apoptosis of ESCC. However, expression of FADD had been variable among ESCC cell lines and its role as an adapter protein for TRAIL receptors remained unclear. Recently, activation of the intrinsic pathway in TRAIL-mediated apoptosis has been described; Bax seems to take a critical pro-apoptotic role while Bcl-XL is an important inhibitory factor in this pathway of

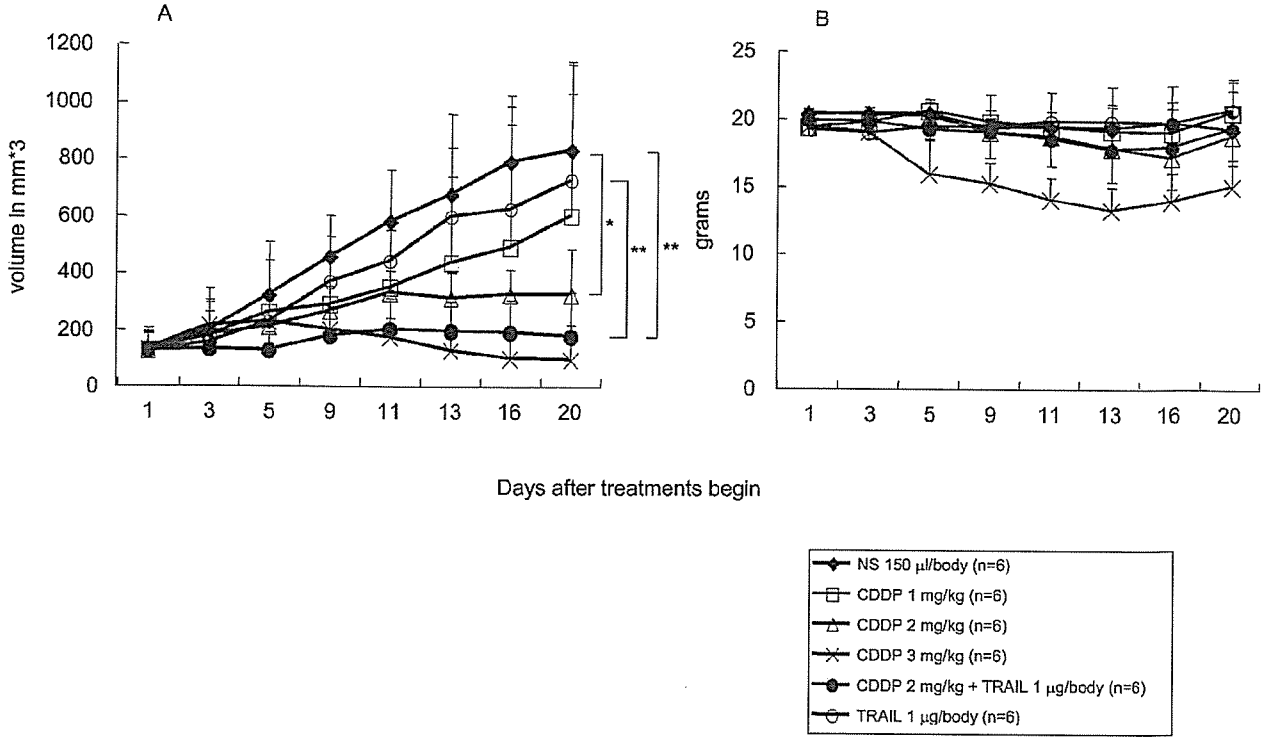

FIGURE 10 – Synergistic antitumor effect of the combination treatment with TRAIL and cisplatin *in vivo*. (*a*) KYSE 170 cells (5×10^6) were inoculated into the right thigh of Balb/c nude mice. After tumor formation, mice received i.p. injection of either TRAIL, cisplatin, normal saline or the combination of TRAIL (1 µg/body) and cisplatin (2 mg/kg). Cisplatin alone induced dose-dependent suppression of xenografted tumor growth, although low-dose cisplatin (1 mg/kg) was largely ineffective. The combination treatment resulted in statistically significant tumor growth suppression compared to both the control and TRAIL-alone groups. (*b*) injection of TRAIL alone resulted in no weight loss of nude mice, while cisplatin caused weight loss of nude mice in a dose-dependent manner. Weight loss was particularly prominent when 3 mg/kg cisplatin was administered. Closed circle, Control group with normal saline; open circle, TRAIL (1 µg/body); open square, cisplatin (1 mg/kg); open triangle, cisplatin (2 mg/kg); ×, cisplatin (3 mg/kg); closed circle, TRAIL (1 µg/kg) + cisplatin (2 mg/kg). Data are shown as the means; bars, SE. $*p < 0.05$. $**p < 0.001$.

apoptosis.[38–42] We detected varying levels of Bax and Bcl-XL in 8 KYSE cell lines but the evidence for the intrinsic pathway activation in the sensitive cell lines could not be obtained. Meanwhile, detection of anti-apoptotic proteins by Western blotting disclosed slight decreases in FLIPS and XIAP expression in the combination-treatment sensitive cell lines after the treatment with 5 µg/ml cisplatin. Such changes were not observed in the resistant KYSE cell lines. FLIP blocks the binding of caspase-8 to the death domains of DR to inhibit apoptosis induction and has been shown to be critical in TRAIL resistance of other cancers,[13,34,43,44] while XIAP inhibits the intrinsic pathway of apoptosis.[45] Cisplatin-mediated decreases of these 2 proteins might partially explain the cell lines' sensitivity to the combination treatment. However, more definitive intracellular mechanisms that determine ESCC's sensitivity to TRAIL and cisplatin are likely to exist, and this shall be the topic of further study. On the contrary, Western blotting did not prove any significant changes in the NFκB expression levels after the cisplatin treatment in any of the cell lines. While NFκB is generally considered anti-apoptotic,[11,46] a moderate amount of activated NFκB has been suggested to upregulate DRs.[22] Subsequently, it will be necessary to detect the active form of NFκB to evaluate its roles in DR upregulation of ESCC.

Importantly, pretreatment of KYSE cell lines with cisplatin followed by TRAIL resulted in significant cytotoxic effects compared to the reverse sequence in the treatment-sensitive KYSE cell lines, thus supporting the significance of cisplatin-induced upregulation of DRs. Furthermore, *in vivo* experiments with nude mice revealed synergistic effects of the combination treatment similar to *in vitro* results when compared to the TRAIL-alone (1 µg/body) group. Although statistical significance was not reached when compared to cisplatin-alone group (2 mg/kg), tendency toward synergy was observed; an encouraging outcome that may lead to further investigation. Notably, we were able to obtain these results with much lower dose of TRAIL than previously reported.[19,32] Growth of the xenografted KYSE 170 was suppressed by administration of cisplatin alone even though this cell line was resistant to cisplatin *in vitro*. We believe this seemingly discrepant result was obtained probably because with the administration of the given concentration of cisplatin, the serum concentration became sufficiently high to cause some apoptosis. TRAIL was shown to have negligible influences on weight loss at 1 µg/body, implying minimal side effects.

These results support the cisplatin-dependent DR upregulation as a critical factor in augmenting TRAIL-mediated apoptosis in ESCC and in addition may provide the following clinical implication: first, there is a possibility that the combination therapy can overcome not only TRAIL resistant but also cisplatin resistant ESCC. Second, synergistic effects of the combination treatment against ESCC obtained *in vitro* can be translated into *in vivo* experiments. Third, in the clinical settings, sequential administration of cisplatin and TRAIL, which may be safer, might be the better way of treating the patients. Since the critical issue regarding toxicity of recombinant human TRAIL to normal human cells appeared to be resolved by alternating its

formulation,[17,18] TRAIL shall remain as a feasible candidate for anticancer therapies. While testing for clinical application of the recombinant human TRAIL against many different cancers is presently under intense investigation, research on TRAIL against ESCC has been limited. We attempted to show such a possibility, and it is our hope that continuing researches may eventually lead to the introduction of TRAIL as the standard agent for anti-esophageal cancer therapy.

References

1. Wiley RS, Schooley K, Smolak PJ, Din WS, Huang C-P, Nicholl JK, Sutherland GR, Smith TD, Rauch C, Smith CA, Goodwin RG. Identification and characterization of a new member of the TNF family that induces apoptosis. Immunity 1995;3:673–82.
2. Pitti RM, Marsters SA, Ruppert S, Donahue CJ, Moore A, Ashkenazi A. Induction of apoptosis by Apo-2 ligand, a new member of the tumor necrosis factor cytokine family. J Biol Chem 1996;271:12687–90.
3. Pan G, O'Rourke K, Chinnaiyan AM, Gentz R, Ebner R, Ni J, Dixit VM. The receptor for the cytotoxic ligand TRAIL. Science 1997; 276:111–3.
4. Schneider P, Bodmer J-L, Thome M, Hofmann K, Holler N, Tschopp J. Characterization of two receptors for TRAIL. FEBS Lett 1997; 416:329–34.
5. Sheridan JP, Marsters SA, Pitti RM, Gurney A, Skubatch M, Baldwin D, Ramakrishnan L, Gray CL, Baker K, Wood WI, Goddard AD, Godowski P, et al. Control of TRAIL-induced apoptosis by a family of signaling and decoy receptors. Science 1997;277:818–21.
6. Pan G, Ni J, Wei Y-F, Yu G-L, Gentz R, Dixit VM. An antagonist decoy receptor and a death domain-containing receptor for TRAIL. Science 1997;277:815–8.
7. Walczak H, Degli-Esposti MA, Johnson RS, Smolak PJ, Waugh JY, Boiani N, Timour MS, Gerhart MJ, Schooley KA, Smith CA, Goodwin RG, Rauch CT. TRAIL-R2: a novel apoptosis-mediating receptor for TRAIL. EMBO J 1997;16:5386–97.
8. Chaundhary PM, Eby M, Jasmin A, Bookwalter A, Murray J, Hood L. Death receptor 5, a new member of the TNFR family, and DR4 induce FADD-dependent apoptosis and activate the NF-κB pathway. Immunity 1997;7:821–30.
9. Marsters SA, Sheridan JP, Pitti RM, Huang A, Skubatch M, Baldwin D, Yuan J, Gurney A, Goddard AD, Godowski P, Ashkenazi A. A novel receptor for Apo2L/TRAIL contains a truncated death domain. Curr Biol 1997;7:1003–6.
10. Pan G, Ni J, Yu G-L, Wei Y-F, Dixit VM. TRUNDD, a new member of the TRAIL receptor family that antagonizes TRAIL signaling. FEBS Lett 1998;424:41–5.
11. Degli-Esposti MA, Dougall WC, Smolak PJ, Waugh JY, Smith CA, Goodwin RG. The novel receptor TRAIL-R4 induces NF-κB and protects against TRAIL-mediated apoptosis, yet retains an incomplete death domain. Immunity 1997;7:813–20.
12. Jo M, Kim T-H, Seol D-W, Esplen JE, Dorko K, Billiar TR, Strom SC. Apoptosis induced in normal human hepatocytes by tumor necrosis factor-related apoptosis-inducing ligand. Nat Med 2000;6: 564–7.
13. Kim K, Fisher MJ, Xu S-Q, El-Deiry WS. Molecular determinants of response to TRAIL in killing of normal and cancer cells. Clin Cancer Res 2000;6:335–46.
14. Keane MM, Ettenberg SA, Nau MM, Russell EK, Lipkowitz S. Chemotherapy augments TRAIL-induced apoptosis in breast cancer cell lines. Cancer Res 1999;59:734–41.
15. Griffith TS, Rauch CT, Smolak PJ, Waugh JY, Boiani N, Lynch DH, Smith CA, Goodwin RG, Kubin MZ. Functional analysis of TRAIL receptors using monoclonal antibodies. J Immunol 1999;162:2597–605.
16. Leverkus M, Neumann M, Mengling T, Rauch CT, Brocker E-B, Krammer PH, Walczak H. Regulation of Tumor necrosis factor-related apoptosis-inducing ligand sensitivity in primary and transformed human keratinocytes. Cancer Res 2000;60:553–9.
17. Qin J-Z, Chaturvedi V, Bonish B, Nickoloff BJ. Avoiding premature apoptosis of normal epidermal cells. Nat Med 2001;7:385–6.
18. Lawrence D, Shahrokh Z, Marsters S, Achilles K, Shih D, Mounho B, Hillan K, Totpal K, DeForge L, Schow P, Hooley J, Sherwood S et al. Differential hepatocyte toxicity of recombinant Apo2L/TRAIL versions. Nat Med 2001;7:383–85.
19. Nagane M, Pan G, Weddle JJ, Dixit VM, Cavenee WK, Su Huang H-J. Increased death receptor 5 expression by chemotherapeutic agents in human gliomas causes synergistic cytotoxicity with tumor necrosis factor-related apoptosis-inducing ligand in vitro and in vivo. Cancer Res 2000;60:847–53.
20. Eggert A, Grotzer MA, Zuzak TJ, Wiewrodt BR, Ho R, Ikegaki N, Brodeur GM. Resistance to Tumor necrosis factor-related apoptosis-inducing ligand-induced apoptosis in neuroblastoma cells correlates with a loss of caspase-8 expression. Cancer Res 2001;61:1314–9.
21. Naka T, Sugamura K, Hylander BL, Widmer MB, Rustum YM, Repasky EA. Effects of tumor necrosis factor-related apoptosis-inducing ligand alone and in combination with chemotherapeutic agents on patients' colon tumors grown in SCID mice. Cancer Res 2002;62: 5800–6.
22. Gibson SB, Oyer R, Spalding AC, Anderson SM, Johnson GL. Increased expression of death receptors 4 and 5 synergizes the apoptosis response to combined treatment with etoposide and TRAIL. Mol Cell Biol 2000;20:205–12.
23. Hopkins-Donaldson S, Bodmer J-L, Bourloud KB, Brognara CB, Tschopp J, Gross N. Loss of caspase-8 expression in highly malignant human neuroblastoma cells correlates with resistance to tumor necrosis factor-related apoptosis-inducing ligand-induced apoptosis. Cancer Res 2000;60:4315–9.
24. Shimada Y, Imamura M, Wagata T, Yamaguchi N, Tobe T. Characterization of 21 newly established esophageal cancer cell lines. Cancer 1992;69:277–84.
25. Kanda Y, Nishiyama Y, Shimada Y, Imamura M, Nomura H, Hiai H, Fukumoto M. Analysis of gene amplification and overexpression in human esophageal-carcinoma cell lines. Int J Cancer 1994;58:291–7.
26. Yu R, Mandlekar S, Ruben S, Ni J, Kong A-NT. Tumor necrosis factor-related apoptosis-inducing ligand-mediated apoptosis in androgen-independent prostate cancer cells. Cancer Res 2000;60:2384–9.
27. Grusch M, Fritzer-Szkeres M, Fuhrmann G, Rosenberger G, Luxbacher C, Elford HL, Smid K, Peters GJ, Szekeres T, Krupitza G. Activation of caspases and induction of apoptosis by novel ribonucleotide reductase inhibitors amidox and didox. Exp Hematol 2001; 29:623–32.
28. Miyahara T, Ueda K, Akaboshi M, Shimada Y, Imamura M, Utsumi H. Hyperthermic enhancement of cytotoxicity and increased uptake of cis-diamminedichloroplatinum(II) in cultured human esophageal cancer cells. Jpn J Cancer Res 1993;84:336–40.
29. Griffith TS, Chin WA, Jackson GC, Lynch DH, Kubin MZ. Intracellular regulation of TRAIL-induced apoptosis in human melanoma cells. J Immunol 1998;161:2833–40.
30. Korsmeyer SJ, Wei MC, Saito M, Weiler S, Oh KJ, Schlesinger PH. Pro-apoptotic cascade activates BID, which oligomerizes BAK or BAX into pores that result in the release of cytochrome c. Cell Death Diff 2000;7:1166–73.
31. Li H, Zhu H, Xu CJ, Yuan J. Cleavage of BID by caspases 8 mediates the mitochondrial damage in the Fas pathway of apoptosis. Cell 1998;94:491–501.
32. Singh TR, Shankar S, Chen X, Asim M, Strivastava RK. Synergistic interactions of chemotherapeutic drugs and Tumor Necrosis Factor-related apoptosis-inducing ligand/Apo-2L ligand on apoptosis and on regression of breast carcinoma in vivo. Cancer Res 2003;63:5390–400.
33. Yamanaka T, Shiraki K, Sugimoto K, Ito T, Fujikawa K, Ito M, Takase K, Moriyama M, Nakano T, Suzuki A. Chemotherapeutic agents augment TRAIL-induced apoptosis in human hepatocellular carcinoma cell lines. Hepatology 2000;32:482–90.
34. Sheikh MS, Burns TF, Huang Y, Wu GS, Amundson S, Brooks KS, Fornace AJ Jr., El-Deiry WS. p53-dependent and -independent regulation of the death receptor KILLER/DR5 gene expression in response to genotoxic stress and tumor necrosis alpha. Cancer Res 1998;58: 1593–8.
35. Nimmanapalli R, Perkins CL, Orlando M, O'Bryan E, Nguyen D, Bhalla KN. Pretreatment with paclitaxel enhances apo-2 ligand/tumor necrosis factor-related apoptosis-inducing ligand-induced apoptosis of prostate cancer cells by inducing death receptors 4 and 5 protein levels. Cancer Res 2001;61:759–63.
36. Zhang XD, Franco AV, Nguyen T, Gray CP, Hersey P. Differential localization of death and decoy receptors for TNF-related apoptosis-inducing ligand (TRAIL) in human melanoma cells. J Immunol 2000;164:3961–70.
37. Griffith TS, Fialkov JM, Scott DL, Azuhata T, Williams RD, Wall NR, Altieri DC, Sandler AD. Induction and regulation of tumor necrosis factor-related apoptosis-inducing ligand/Apo-2 ligand-mediated apoptosis in renal cell carcinoma. Cancer Res 2002;62:3093–9.
38. Suliman A, Lam A, Datta R, Strivastava RK. Intracellular mechanism of TRAIL: apoptosis through mitochondrial-dependent and -independent pathways. Oncogene 2001;20:2221–33.
39. Ravi R, Bedi A. Requirement of BAX for TRAIL/Apo2L-induced apoptosis of colorectal cancers: synergism with Sulindac-mediated inhibition of Bcl-XL. Cancer Res 2002;62:1583–7.
40. Kim J-Y, Kim Y-H, Chang I, Kim S, Pak YK, Oh B-H, Yagita H, Jung YK, Oh YJ, Lee M-S. Resistance of mitochondrial DNA-defi-

cient cells to TRAIL: role of Bax in TRAIL-induces apoptosis. Oncogene 2001;21:3139–48.
41. Sarker M, Ruiz-Ruiz C, Robledo G, López-Rivas A. Stimulation of the mitogen-activated protein kinase pathway antagonizes TRAIL-induced apoptosis downstream of BID cleavage in human breast cancer MCF-7 cells. Oncogene 2002;21:4323–27.
42. Wolter KG, Hsu Y-T, Smith CL, Nechushtan A, Xi X-G, Youle RJ. Movement of Bax from the cytosol to mitochondria during apoptosis. J Cell Biol 1997;139:1281–92.
43. Kim JH, Ajaz M, Lokshin A, Lee YJ. Role of antitpoptotic proteins in Tumor Necrosis Factor-related Apoptosis-inducing Ligand and Cisplatin-augmented apoptosis. Clin Cancer Res 2003;9:3134–41.
44. Nam SY, Jung G-A, Hur G-C, Chung H-Y, Kim WH, Seol D-W, Lee BL. Upregulation of FLIPs by Akt, a possible inhibition mechanism of TRAIL-induced apoptosis in human gastric cancers. Cancer Sci 2003;94:1066–73.
45. Fulda S, Meyer E, Debatin K-M. Inhibition of TRAIL-induced apoptosis by Bcl-2 overexpression. Oncogene 2002;21:2283–94.
46. Franco AV, Zhang XD, Berkel EV, Sanders JE, Zhang XY, Thomas WD, Nguyen T, Hersey P. The role of NF-κB in TNF-related apoptosis-inducing ligand (TRAIL)-induced apoptosis of melanoma cells. J Immunol 2001;166:5337–45.

Esophageal Cancer: Evaluation with Triple-Phase Dynamic CT—Initial Experience[1]

Shigeaki Umeoka, MD
Takashi Koyama, MD, PhD
Kaori Togashi, MD, PhD
Tsuneo Saga, MD, PhD
Go Watanabe, MD, PhD
Yutaka Shimada, MD, PhD
Masayuki Imamura, MD, PhD

Purpose: To prospectively assess which phase of a triple-phase dynamic contrast material–enhanced multi–detector row computed tomography (CT) protocol is optimal for visualization of esophageal cancer.

Materials and Methods: The study was supported by the local ethical committee; all patients gave written informed consent. Thirty-one lesions in 28 consecutive patients (26 men, two women; mean age, 65 years; range, 53–87 years) with histopathologically confirmed esophageal cancer were evaluated with triple-phase dynamic CT performed at 5, 35, and 65 seconds (first arterial, second arterial, and venous phases) after attenuation of 200 HU was obtained at the descending aorta. Qualitative image analysis was performed to assess appearance and conspicuity of the tumor. Appearances of all 31 lesions were classified into three categories—not identifiable, focal enhancement with or without minimal (<1 cm) wall thickening, and focal mass lesion or obvious (>1 cm) wall thickening. Results were compared with surgical or endoscopic ultrasonographic findings. Quantitative assessment included regions-of-interest measurement of the tumor and normal esophageal wall and the difference between those measurements. A paired *t* test was used to determine which phase showed the highest tumor attenuation and tumor-to-normal esophageal wall attenuation differences.

Results: At visual assessment, 30 lesions were identified in the second arterial phase. Of these 30 lesions, eight were focal enhancements; the best conspicuity was during the second arterial phase. Furthermore, seven of these eight lesions were T1 cancers. The remaining 22 lesions were enhanced masses or wall thickening. Twenty-one of these 22 tumors also showed best conspicuity in the second arterial phase. The greatest attenuation of tumors in the second arterial phase was 130.0 HU, and the difference in attenuation between tumor and normal esophageal wall was 50.6 HU in the second arterial phase, which were significantly higher than those in the other two phases ($P < .01$, each).

Conclusion: The second arterial phase of dynamic CT is the optimal phase for visualization of esophageal cancer.

[1] From the Department of Diagnostic Imaging and Nuclear Medicine (S.U., K.T., T.S.) and Department of Surgery and Surgical Basic Science (G.W., Y.S., M.I.), Graduate School of Medicine, Kyoto University, Kyoto, Japan; and Department of Radiology, Kyoto University Hospital, 54 Kawahara-cho, Shogoin, Sakyo, Kyoto, 606-8507, Japan (T.K.). From the 2003 RSNA Annual Meeting. Received February 9, 2005; revision requested April 8; revision received April 28; accepted June 3; final version accepted August 11. **Address correspondence to** T.K. (e-mail: *montpeti@kuhp.kyoto-u.ac.jp*).

Esophageal cancer is one of the common malignant neoplasms in the world. Every year, approximately 13 900 cases of esophageal cancer are diagnosed in the United States, and 13 000 Americans die of it (1). Patients with esophageal cancer generally present with progressive dysphagia, malnutrition, and weight loss. As with other malignant tumors, accurate TNM staging and localization of the esophageal cancer are important parameters for selection of the optimal treatment and for prediction of patients' prognoses.

Small polypoid lesions, plaquelike lesions, focal irregularities of the esophageal wall, and spreading superficial lesions are common findings of early esophageal cancer (2,3). Because some benign esophageal tumors such as squamous papillomas can reveal similar findings, subsequent biopsy with an upper-esophageal endoscopic technique is required to confirm malignancy. A barium swallow examination typically reveals mucosal irregularity or stricture or ulceration of the esophagus. In cases of early and advanced stage esophageal cancer, the TNM stage is determined after histopathologic diagnosis in order to devise therapeutic strategies based on results of multiple imaging studies, including upper gastrointestinal endoscopy, endoscopic ultrasonography (US), computed tomography (CT), and fluorine 18 fluorodeoxyglucose positron emission tomography (4).

Because endoscopic US can depict the normal esophageal wall as a five-layer structure, it can be used to evaluate the depth of tumor extension (5). Although CT has been used for preoperative evaluation of esophageal cancer, the major role of CT has been the depiction of lymph nodes, distant metastases, or both rather than the evaluation of the local status of esophageal cancer. Several studies attempted to use conventional CT to stage esophageal cancer, only to find that CT was useful for evaluating T4 lesions (6–8). The sensitivity of conventional CT protocols in localizing esophageal cancer, especially early stage cancer, is not satisfactory, perhaps because conventional CT cannot afford optimal conspicuity of esophageal cancers against the normal esophageal wall.

Several reports describe potential advantages of CT images obtained during the arterial phase after the administration of contrast material; these images depict gastrointestinal cancers in other organs (9–11). To our knowledge, however, this imaging technique has not been applied to esophageal cancer, as the esophagus is too long to be imaged entirely during the arterial phase at conventional CT. Multi-detector row CT has markedly improved time resolution and permits acquisition of arterial phase images of the entire esophagus during a single breath hold. Thus, the goal of our study was to prospectively assess which phase of a triple-phase dynamic contrast material–enhanced multi-detector row CT protocol is optimal for visualization of esophageal cancer.

Advance in Knowledge

- The second arterial phase of triple-phase dynamic CT is the optimal phase for visualization of esophageal cancer.

Materials and Methods

Patients

Our study population included 31 lesions in 28 consecutive patients (26 men, two women; age range, 53–87 years; mean age, 65 years) with esophageal cancer histopathologically proved at endoscopic biopsy who were referred to our institution for possible surgical treatment from June 2002 to March 2003. Three patients had double primary lesions. All 28 patients underwent CT for local staging of the tumors and for evaluation of lymph nodes and distant metastases. Informed consent, which included regard to radiation dose, was obtained from all 28 patients prior to performance of triple-phase dynamic contrast-enhanced CT, in accordance with a protocol approved by the ethical committee at our institution. Anatomic subsite was divided according to Union Internationale Contre le Cancer classification: cervical esophagus, from the lower border of the cricoid cartilage to the superior thoracic aperture; upper thoracic portion, from the superior thoracic aperture to the level of tracheal bifurcation; midthoracic portion as the proximal half between the tracheal bifurcation and the esophagogastric junction; and lower thoracic portion, as the distal half between the tracheal bifurcation and the esophagogastric junction. The esophageal cancers were in the cervical esophagus in two lesions, the upper thoracic portion in five lesions, the midthoracic portion in eight lesions, both the upper thoracic and midthoracic portions in three lesions, the lower thoracic portion in five lesions, and both the midthoracic and lower thoracic portions in eight lesions. Histopathologic diagnoses were squamous cell carcinoma (30 lesions, 27 patients) and adenocarcinoma arising in a Barrett esophagus (one lesion, one patient). Treatments were the following: surgical resection for 15 lesions in 14 patients, radiation therapy or combined chemotherapy and radiation therapy for seven lesions in five patients, endoscopic mucosal resection for one lesion in one patient, and combination of surgical resection with radiation therapy, chemotherapy, or both in eight lesions in eight patients. The local extent of the primary tumor (T classification) was determined with histopathologic assessment of the resected specimens (23 lesions) according to the TNM classification. For the eight lesions without surgical interven-

Published online before print
10.1148/radiol.2393050222

Radiology 2006; 239:777–783

Abbreviation:
ROI = region of interest

Author contributions:
Guarantor of integrity of entire study, T.K.; study concepts/study design or data acquisition or data analysis/interpretation, all authors; manuscript drafting or manuscript revision for important intellectual content, all authors; approval of final version of submitted manuscript, all authors; literature research, S.U., T.K., K.T.; clinical studies, all authors; statistical analysis, S.U.; and manuscript editing, S.U., T.K., K.T., T.S., M.I.

Authors stated no financial relationship to disclose.

tions, results from endoscopic US were used as the reference standard for diagnosis. The criteria for staging with endoscopic US evaluation were based on the classification system for the esophagus as proposed by the Japanese Society for Esophageal Diseases (12,13).

Dynamic CT Protocol

All examinations were performed with the same multi-detector row CT scanner (Aquilion M8; Toshiba Medical, Tokyo, Japan). CT scans were obtained after intravenous injection of 100 mL of nonionic contrast medium (350 or 370 mg of iodine per milliliter) (Iomeprol, Eisai, Tokyo, Japan; Iopamidol, Nihon Schering, Osaka, Japan) at a rate of 3 mL/sec. Triple-phase imaging with a single breath hold for each phase was automatically performed 5, 35, and 65 seconds (first arterial phase, second arterial phase, and venous phase) after the attenuation of the descending aorta reached 200 HU. The first and second arterial phase acquisitions covered from the neck to the level of the esophagogastic junction, whereas the venous phase acquisitions covered the whole abdominal and pelvic region, in addition to the neck and chest region. Thirty-second intervals were allowed between each phase (15 seconds to obtain images of the entire length of the esophagus and another 15 seconds for patients to recover their breath). Oral esophageal contrast material was not used in this study, because esophageal enhancement may be confused with tumor enhancement on images.

Images were acquired with 1- or 2-mm section thickness, beam collimation of 8, 556-msec rotation time, beam pitch of 1.7 or 0.875, 120 kVp, 300 mA per rotation, and 14-mm table feed per rotation. The thin-section CT data were transferred to a workstation (M900 Quadra; Ziosoft, Tokyo, Japan), and transverse 7.0-mm-thick sections were reconstructed at 7.0-mm intervals. The reconstruction field of view was 320 mm for each section. Multiplanar reformatted images were also reconstructed by one of the authors (S.U., with approximately 5 years of experience in thoracic and abdominal CT) with a 1.0-mm section thickness in the oblique sagittal plane, which included the tumor and either the trachea (in cases of cervical or upper thoracic esophageal cancers) or the descending aorta (in cases of midthoracic or lower thoracic esophageal cancers). Standard mediastinal window images (window width, 400 HU; window level, 60 HU) were used for displaying the images.

Qualitative Analysis

Qualitative image analysis was prospectively performed on both transverse CT images and multiplanar reformatted CT images by two radiologists (T.K. and T.S., each with approximately 9 years of experience in thoracic and abdominal CT) who were aware of the histopathologic diagnosis of esophageal cancer but had no information on numbers and location of the tumor described in the surgical and US endoscopic findings. These readers assessed the images for the presence of the tumor, which is noted as focal enhancement. When the tumor was identified, each reader recorded the location and thickness of the lesion. Discrepancies in assessment were solved by consensus. For each imaging phase, appearances of all 31 lesions were classified into the following three categories: not identifiable (type 1), focal enhancement with or without minimal (<1 cm) wall thickening (type 2), and focal mass lesion or obvious (>1 cm) wall thickening (type 3).

Visual assessment of the phase that best showed the tumor against normal esophageal wall was also performed by using a five-point scale: 1, nonidentifiable; 2, hardly identifiable; 3, adequate; 4, good; and 5, excellent. Conspicuity of a type 1 lesion was equivalent to a score of 1. Conspicuity of type 2 or 3 lesions was ranked according to scores 2–5.

Table 1

Appearance of 31 Esophageal Tumors on Triple-Phase CT Images, according to Imaging Phase

	No. of Detectable Lesions		
Appearance of Esophageal Tumors	First Arterial Phase	Second Arterial Phase	Venous Phase
Not identifiable (type 1)	9	1	7
Focal enhancement with or without minimal (<1 cm) wall thickening (type 2)	0	8	2
Focal mass lesion or obvious (>1 cm) wall thickening (type 3)	22	22	22

Table 2

Best Esophageal Tumor Conspicuity on Triple-Phase CT Images, according to Imaging Phase

	Best Conspicuity			
Appearances of Esophageal Tumors	First Arterial Phase	Second Arterial Phase	Venous Phase	Both Second and Venous Phases
Focal mass lesion or obvious (>1 cm) wall thickening (type 3) ($n = 22$)	0	10	1	11
Focal enhancement with or without minimal (<1 cm) wall thickening (type 2) ($n = 8$)	0	8	0	0

Although histopathologic confirmations were not obtained, linear or punctuate enhancements along the surface mucosa were considered to be physiologic mucosal enhancement or vessels. These enhanced structures were carefully excluded. High attenuation due to beam hardening artifacts at the interface between the esophageal lumen and the esophageal wall were also carefully excluded. The locations of the esophageal cancers at CT assessment were finally compared with surgical or endoscopic findings by another author (S.U.).

Quantitative Analysis

In parallel with qualitative analyses, quantitative analyses were performed by another radiologist (S.U.) who was aware of the tumor locations from endoscopic US or surgical results. The mean attenuations of the esophageal tumor and of the normal esophageal wall were measured in Hounsfield units within three circular regions of interest (ROIs), which were created as large as possible on both the cancerous and the normal esophageal wall on the transverse image. The average of the three measurements was calculated as attenuation of the tumor and attenuation of the normal esophageal wall. When defining all ROIs, the radiologist paid special attention not to include necrosis within the tumor, linear enhancement along the surface mucosa, esophageal contents, fat tissue, or surrounding vessels. If the tumor was not identifiable during one or two imaging phases, the ROI was defined by referring to images of another phase that showed the location of the lesion.

Data and Statistical Analysis

Tumor locations and appearances interpreted from the CT images were compared with surgical and endoscopic US findings. The differences in CT attenuation between the tumor and the normal esophageal wall were calculated as an indicator of visual conspicuity of the lesion. Both attenuation of the tumors and subtracted tumor-to–normal esophageal wall attenuation differences were compared between images from different phases. Paired t tests were performed with statistical software (Stat View version 5.0.1; SAS Institute, Cary, NC). Because data were accumulated over time, a repeated measurement distribution analysis was carried out. Compensation of the multiplex nature was performed by the Tukey method. A P value of less than .05 was considered to indicate a statistically significant difference.

Results

Staging

The local endoscopic US or surgical staging of the 31 lesions included T1 cancer in nine lesions (one T1a, eight T1b), T2 cancer in five lesions, T3 cancer in 12 lesions, and T4 cancer in five lesions.

Figure 1

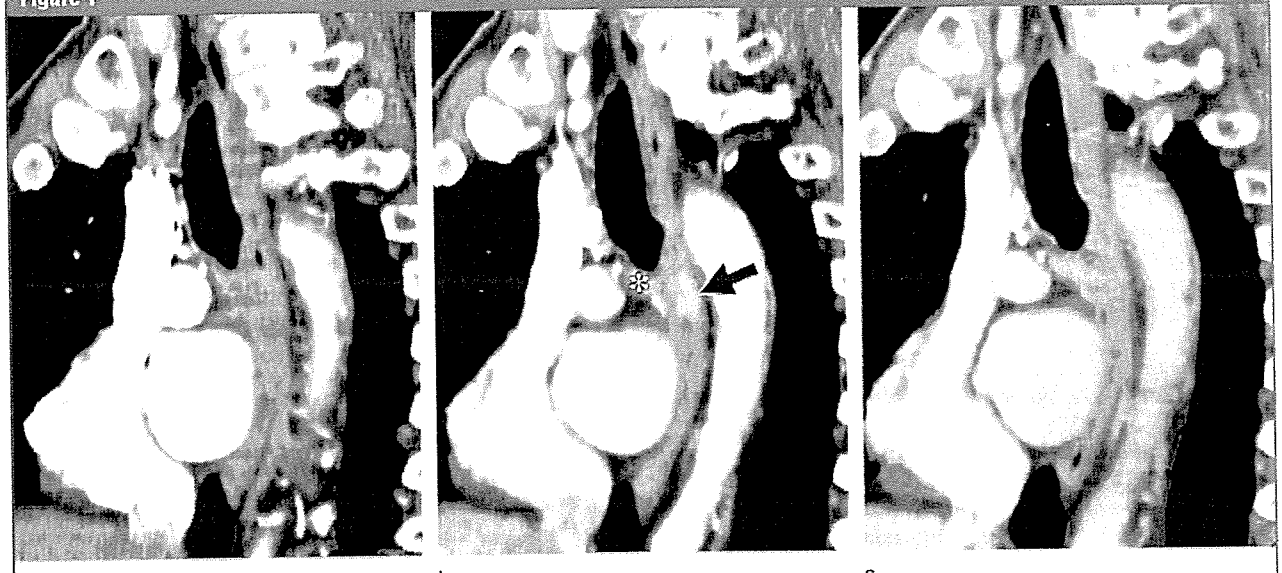

a. b. c.

Figure 1: Oblique sagittal reformatted CT images of 72-year-old man with submucosal esophageal cancer (T1b cancer) 20 × 15 mm in diameter in midthoracic portion. **(a)** First arterial phase image shows smooth esophageal walls without any abnormal enhancement. **(b)** Second arterial phase image reveals focal enhancement (arrow) about 8 mm in diameter and 15 mm in length without any wall thickening (approximately 9 mm thick). Image provides best conspicuity among three phases. Subcarinal adenopathy is seen (*). **(c)** Venous phase image does not show abnormality as well. Average attenuation of tumor is 82 HU in first arterial phase, 129 HU in second arterial phase, and 97 HU in venous phase. Difference in attenuation between tumor and esophageal wall is 10 HU in first arterial phase, 49 HU in second arterial phase, and 5 HU in venous phase.

Figure 2

a. b. c.

Figure 2: Oblique sagittal reformatted CT images of 55-year-old man with T3 tumor of 5.5 cm in diameter in midthoracic portion (small arrows) and T3 tumor of 7.0 cm in diameter in upper thoracic portion (arrowheads). **(a)** First arterial phase image demonstrates tumors in upper and midthoracic portions. **(b)** Second arterial phase image displays an early attenuation of lesions and provides best conspicuity of tumor among the three phases. Lower edge of tumor is clearly identifiable on image (large arrow). **(c)** Venous phase image shows tumors with less conspicuous margins compared with second arterial phase image. Average attenuations of upper thoracic and midthoracic tumors are 83 HU and 89 HU in first arterial phase, 129 HU and 116 HU in second arterial phase, and 116 HU and 112 HU in venous phase, respectively. Tumor-to–normal esophageal wall attenuation differences are 28 HU and 34 HU in first arterial phase, 64 HU and 66 HU in second arterial phase, and 44 HU and 40 HU in venous phase, respectively.

Qualitative Analysis

The presence of all esophageal cancers depicted at CT had been correctly determined from the surgical specimens or endoscopic US. At CT, thirty lesions (97%), which included three skip lesions, were identifiable in the second arterial phase, whereas 22 lesions (71%) were identifiable in the first arterial phase and 24 lesions (77%) were identifiable in the venous phase (Table 1). Only one lesion (type 1) was not identifiable at CT during any of the three phases; this lesion was an adenocarcinoma arising in a Barrett esophagus. At histopathologic examination, the tumor was confined to the mucosal layer within the Barrett epithelium (T1a cancer). The mean wall thickness of the 30 identifiable tumors was 12 mm.

The appearances of eight lesions were interpreted as type 2 cancers on second arterial phase images. Seven of these eight lesions (88%) were histopathologically diagnosed as T1b tumors, whereas the remaining lesion was diagnosed as T2 cancer. Of these eight lesions, none were identifiable in the first arterial phase, and only two lesions were depicted in the venous phase. All eight lesions were depicted most conspicuously in the second arterial phase (Table 2), and six lesions were identifiable only in the second arterial phase (Fig 1).

Twenty-two lesions had type 3 appearances and were identifiable in all three phases (Fig 2). These 22 lesions consisted of one T1b lesion, four T2 lesions, 12 T3 lesions, and five T4 lesions. In 21 of 22 lesions (95%), the best conspicuity between the tumor and the normal esophageal wall was obtained in the second arterial phase (Table 2). The mean wall thickness of eight type 2 lesions was 6.3 mm, whereas that of the 22 type 3 lesions was 13 mm.

Quantitative Analysis

In 28 of 31 lesions, attenuation was measured. In the remaining three lesions, attenuation could not be measured because one lesion was not identifiable in all three phases and the remaining two lesions were too small to define ROIs within the tumors. The mean attenuation of the esophageal tumor was statistically highest in the second arterial phase ($P < .01$ compared with both the first arterial and the venous phases) (Table 3). With regard to the attenuation difference between the tumor and normal esophagus wall, the second arterial phase also showed significantly better conspicuity than both the first arterial and the venous phases ($P < .01$). The mean attenuation of the esophageal tumor showed a peak in the second arterial phase, while the attenuation of the normal esophageal wall tended to gradually enhance (Fig 3).